ARTICLE | Article in Press

Mechanical, durability, and microstructural performance of biochar-modified concrete using faecal sludge–derived biochar

Raghuvesh Tiwari · Priyansha Mehra · Shaik Hussain · Sanchit Anand

Received: 17 December 2025 / Accepted: 11 August 2026

Abstract
This research explores the potentiality of biochar derived from faecal sludge collected at faecal sludge treatment plants (FSTP) by partially replacing cements used in concrete applications. These plants collect, treat, and manage human waste from septic tanks and sanitation systems. This study focuses on determining the optimal dose of biochar as application for concrete's mechanical, durability properties, and microstructural changes. The biochar's pozzolanic activity was evaluated through the strength activity index, while parameters such as shrinkage, compressive strength, flexural strength, water absorption, and porosity were also measured to gauge its impact on concrete performance. Results indicate that incorporating biochar at specific dosages at 5% and 10% replacement yields significant improvements in concrete properties. After a 91-day curing period, concrete with a 10% biochar substitution demonstrated a 21% increase in compressive strength and a 42% increase in flexural strength, highlighting biochar's contribution to mechanical performance. Water absorption and porosity values for concrete with a 15% biochar content were found to be comparable to those of conventional control mixes after 28 days of curing. We have observed that after 120 days, the drying shrinkage observed in a 10% biochar mortar mix was like that in ordinary Portland cement (OPC) mortar, indicating the potential of biochar to maintain dimensional stability over extended periods. The reduction in heavy metal concentration in the concrete specimens due to the increased biochar content was also noticed. This result successfully demonstrates, it is helpful to sustain environment by potentially lowering the leaching of harmful substances.

Keywords Biochar · Concrete · Drying shrinkage · Mechanical strength · Industrial solid waste · Cleaner production

Abbreviations

AAS	Atomic absorption spectroscopy
ASTM	American society for testing and materials
C-A-S-H	Calcium–alumino–silicate–hydrate
CH	Calcium hydroxide or portlandite [Ca $(OH)_2$]
C-S-H	Calcium–silicate–hydrate
DTG	Differential thermogravimetry

This Article in Press is shared early to give you faster access to new research. It is citable and carries a permanent DOI. The final edited version will replace it automatically.

https://doi.org/10.1038/s41598-026-66956-6

Published online: 05 September 2026

EDS/EDX	Energy-Dispersive X-ray spectroscopy
EN	European standard
FSTP	Faecal sludge treatment plant
FT-Ir	Fourier transform infrared spectroscopy
IS	Indian standard
ITZ	Interfacial transition zone
OPC	Ordinary portland cement
PSA	Particle size analysis
SEM	Scanning electron microscopy
SEM–EDS/EDX	Scanning electron microscopy coupled with energy-dispersive X-ray spectroscopy
SICART	Sophisticated instrumentation centre for applied research and testing
SAIF	Sophisticated analytical instrument facility
SMD	Sauter mean diameter
TGA	Thermogravimetric analysis
VMD	Volume mean diameter
w/b	Water-to-binder ratio (by mass)
w/c	Water-to-cement ratio (by mass)
XRD	X-ray diffraction
XRF	X-ray fluorescence

Standard cement chemistry abbreviations

A	Aluminum oxide (Al_2O_3)
C	Calcium oxide (CaO)
CH	Calcium hydroxide [$Ca(OH)_2$]
F	Ferric oxide (Fe_2O_3)
H	Water (H_2O)
S	Silicon dioxide (SiO_2)

Introduction

Globally, the expansion of the construction industry is driving an ever-increasing demand for futuristic and advanced infrastructure. However, it is one of the sectors responsible for the maximum CO_2 emissions and depletion of natural resources. Cement, a key ingredient for any construction, where manufacturing process consumes intensive energy and releases high amounts of CO_2. One ton of CO_2 is released into the atmosphere by manufacturing same amount of cement[1]. The CO_2 emissions is contributing 5%- 8% of global emission[2–5]. The life cycle process of cement include such as mining, processing and transportation , increasing greenhouse gases, which affects environmental system[6]. Several studies have been successfully demonstrated to replace cement partially and, in rare cases, fully, to regulate the environmental issues related to cement production. Construction industry are eagerly looking for partially substitute of cement using pozzolanic or supplementary cementitious material (SCM)[7,8]. For instance, the more commonly said pozzolanic materials for cement replacement includes such as fly ash[9], ground granulated blast furnace slag[10], pumice powder[11], rice husk ash[11], metakaolin[12], marble dust[13], silica fume[14]. In addition, agricultural waste[15] and several agricultural ashes such as bagasse ash[16], rice husk ash[17–19], and corn straw ash[20] exhibit similar pozzolanic characteristics and are gaining attention as sustainable alternatives. A material is pozzolanic when a siliceous or siliceous-aluminous substance is finely powdered, it combines with the undesired $Ca(OH)_2$ produced by the cement hydration to produce more potent cementitious binding compounds such as calcium silicate hydrates (C–S–H) and calcium aluminate silicate hydrates

(C–A–S–H)[21,22]. Available pozzolanic materials are not enough to fulfil the huge demand for cement in concrete, and because of their limitations related to cost and compatibility with cement, researchers are looking forward to justifying more promising and eco-friendly replacements. To mitigate the severe consequences of climate change globally, many nations have set limitations in order to reduce carbon emissions.[23]. Biochar is foremost in this queue, produced by burning an organic substance in the complete absence or under a minimal amount of oxygen, resulting in a carbon-rich material[24]. As the resulting material is low in H/C and O/C ratio, it has a better degree of chemical stability and carbonization[25]. Amongst various biomass materials available to produce biochar, the ones that are prominently used such as sawdust waste, bamboo, rice husk, groundnut shell waste, peanut shell, tomato plant waste, castor plant, sugarcane, cow dung, poultry manure, corncob, sludge, grass straw, and human waste[26,27]. In a recent study, Olaiya et al. (2025) investigated the partial replacement of cement with banana leaf ash (BLA) and sawdust ash (SDA)[28]. Consumption of biochar is mostly for soil remediation to improve the health of soil in terms of fertility and as a sorbent for soil contaminated by heavy metals[29]. There are studies inferring that biochar has the potential to store and fix carbon in a stable form in soil[29–31]. Using biochar as a cementitious material offers more opportunity for carbon sequestration and consequently reduces the emission of greenhouse gases[32]. Although there is a dearth of sufficient literature to encompass the guidelines and framework for the potential use of biochar in place of cement to some extent, from recent studies[32,33]. It has been proved that biochar has the potential to be used as one of the sustainable materials for the cementitious industry[34–37]. Few studies have also explored the possibility of biochar as a suitable additive in pavement[38]. Biochar's ability to hold water leads to a stiffer mix initially, while the retained water later contributes to internal curing during the cement hydration process[39]. Ferro and Restucciaand[36] suggested that by adding biochar produced from hazelnut shells (0.80-1% weight of cement), the hardened cement paste has shown improvement in fracture energy and modulus of rupture by 22.20% and 61%, respectively. Choi et al.[39] reveal that replacing 5% of the cement with biochar (by weight) has increased the 28-day compressive strength of mortar by roughly 10%. However, biochar-mortar has a poor flowability as the replacement rate increases; the authors also deduced a reduction of flow by 3%, 17%, and 20% for 5%, 10%, and 15% replacement by weight of cement, respectively. Praneeth et al.[40] studied the impact of biochar produced from corn stover on the carbon dioxide adsorption potential of cement composites, also studied the compressive strength of the bricks before and after carbonation. In a study[41], biochar from sawdust pyrolyzed at 500°C has been used as a cementitious material, and the influence of grain size distribution on the permeability and the hydration has been studied. Gupta and Kua[42] measured the degree of hydration, permeability, along with compressive strength of the mortar mixes and concluded that the mixed saw dust resulted in 10-12% more degree of hydration, which further improved the permeability and compressive strength of the mixes. Gupta et al.[43] studied the influence of biochar from wood waste pyrolyzed at 300^0C and 500^0C temperatures. The study is measuring the permeability, mechanical strength, and drying shrinkage of the concrete. This research concluded that the compressive strength of the mixes enhanced by incorporating 1 and 2% of biochar by weight of cement, there has not been any significant improvement in the modulus of elasticity, flexural strength, and the dry shrinkage of the concrete mixes. Sirico et al.[44], biochar produced from wood chips pyrolyzed nearly 500^0C to study the mechanical properties of mortar mixes, the compressive strength has been slightly reduced with increasing percentage of biochar, optimum dosage in terms of flexural strength was observed at 1% by weight of cement. Patel et al.[45] reported an approximate 20% improvement in compressive strength and concluded that a 2% biochar replacement level is optimal for strength enhancement. The authors[46] concluded that, even if the parameters of the production process are not optimum, produced biochar can be used in cement composites due to its effectiveness; biochar extracted by pyrolysis of woody biomass increased in compressive strength by 16% and 9% for 0.5% and 2% dosages, respectively. In a recent study, predictive models were developed using linear regression and gene expression programming (GEP) to estimate the compressive strength of concrete incorporating olive pit biochar (2.5–5 wt.%)[47]. The experimental results indicated that 2.5 wt.% biochar yielded the highest compressive strength, while 5 wt.% provided optimal tensile and flexural strengths. The GEP model outperformed the linear regression model, highlighting the potential of biochar to produce sustainable, low-carbon concrete with enhanced mechanical performance. Gupta et al.[48] studied the reason for the increase in the compressive strength to the reduction in permeability of concrete samples incorporated with biochar. Bamboo biochar, micro-sized, improved the flexural strength, compressive strength, and toughness of the concrete mix when the dosage of biochar was 0.05-0.2%[49]. A significant and often-overlooked application of biochar was recently investigated by Galano et al.[50], their study explored the self-healing potential of concrete in the presence of calcite-precipitating bacteria (*Bacillus subtilis*, *Bacillus megaterium*, etc.). The research found that this method successfully restored and even improved the strength of cracked specimens, offering a low-cost and environmentally friendly alternative for enhancing concrete durability. Safe disposal of human waste has been a great concern for society to handle. In the past decade, several Faecal Sludge Treatment Plants (FSTP) have been set up and are operational in India. There is ensured disposal of sludge at the FSTP, where raw sludge is processed to generate biochar through pyrolysis, during pyrolysis oil and gases may also be collected[51].

Research gap

Despite growing interest in biochar as a sustainable construction material, the utilization of biochar derived specifically from faecal sludge treatment plants (FSTPs) remains inadequately explored. Currently number of studies and methods available on agricultural or woody biochar, with limited attention to sludge-based biochar, particularly regarding detailed mechanical, durability performance, and potential environmental risks such as heavy metal presence. There is a lack of systematic approaches to optimize biochar incorporation in concrete and to establish clear relationships between biochar content and concrete performance. To address these gaps, the present study investigates the optimum utilization of biochar derived from an FSTP in concrete. The performance of biochar-modified concrete is evaluated against a control mix through comprehensive experimental investigations, including mechanical and microstructural analysis. Response Surface Methodology (RSM) model is developed to optimize mix parameters and quantify the influence of biochar on key concrete properties. This integrated approach aims to provide both experimental evidence and predictive capability, thereby contributing toward the practical implementation of sludge-derived biochar in sustainable construction.

Materials characterisation and design mix proportions

Cement and aggregate

Ordinary Portland Cement (OPC) of 43 grade, manufactured by Ultratech cement company, was used in the current experimental work. Table 1 shows the laboratory tests performed on cement and to study a normal consistency, specific gravity, initial and final setting times as per Indian Standards norms with the physical characteristics. Chemical composition and clinker compounds composition of the OPC used in the study are tabulated in Table 2.

Locally available river sand with particle size up to 4.75mm pertaining to Zone II as per IS 383[53], was used as a fine aggregate. The workflow is presented using flow chart in Fig. 1.

The fineness modulus of fine aggregate was measured to be 2.5 and the gradation curve (Fig. 2a) showing well graded particle distribution which impacts shrinkage, workability, and durability of concrete and mortar**.** Crushed

Table 1 Physical characteristics of cement.

Physical characteristics	OPC	Test standard
Specific gravity	3.15	IS 4031 (Part XI)[52]
Bulk density	1.43 gm/cm^3	
Initial setting time of cement	74 mins	IS: 4031 (Part V)[52]
Final setting time of cement	480 mins	
Normal consistency	31%	IS: 4031 (Part IV)[52]

Table 2 Chemical composition of OPC (%).

Material	Chemical composition							Clinker composition			
	CaO	SiO_2	Al_2O_3	SO_3	Fe_2O_3	MgO	LOI	C_3S	C_2S	C_3A	C_4AF
OPC	60.2	19.4	5.3	2.2	3.2	22.5	1.8	51.11	17.14	8.64	9.73

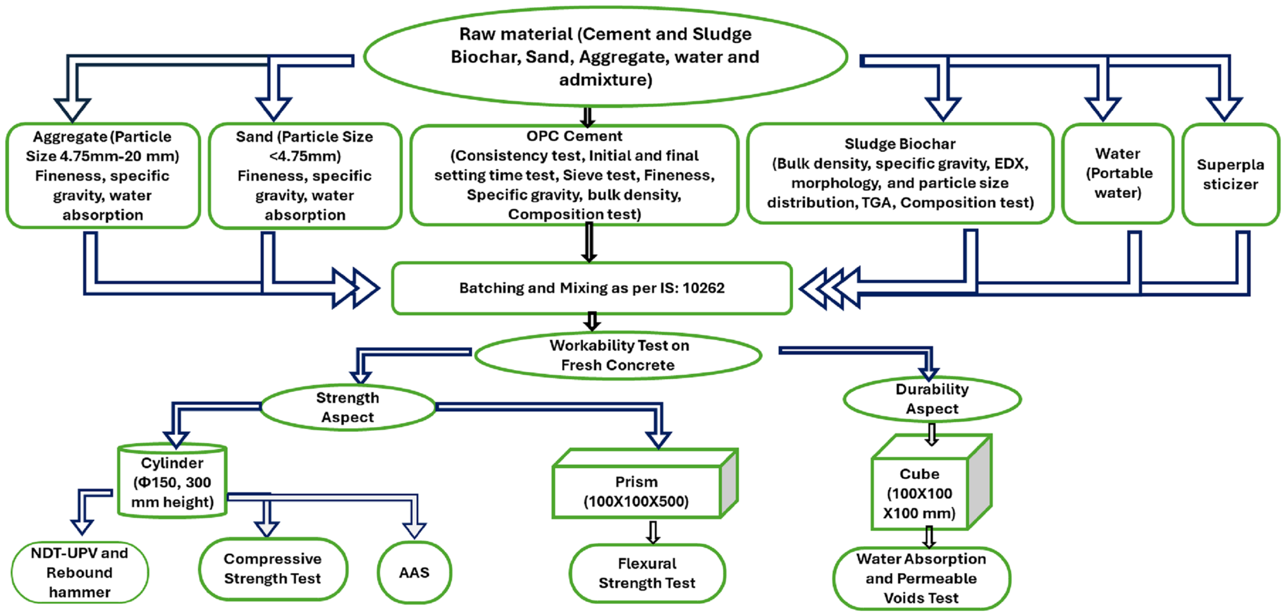

Fig. 1 Typical workflow illustration.

basalt of sizes larger than 4.75 mm up to 20mm from the Aasalpur area Jobner mine was used as coarse aggregate (Fig. 2b). The specific gravity of the fine and coarse aggregates was determined in accordance with IS: 2386 (Part-III) [54], found to be 2.64 and 2.72 respectively.

Biochar and its physicochemical characterization

The biochar used in this study was sourced from the faecal sludge treatment plant (FSTP) at the Site Sanitation Resource Park, Warangal, Telangana. In order to prepare sludge biochar, it was air-dried which was then placed in an oven at 105 ± 5 °C for 24 hours to achieve a constant mass. Controlled pyrolysis process was performed in a muffle furnace under limited oxygen conditions. The dried sludge was heated at a temperature of 350-450°C with a heating rate of approximately 10 °C/min and maintained at peak temperature for 2 hours to ensure complete carbonization. After pyrolysis, the material was allowed to cool naturally inside the furnace to prevent oxidation. The raw sludge biochar (Fig. 3a) was now processed in lab through grinding, sieving and subsequently characterized for its mechanical and microstructural properties.

Bulk density, specific gravity, water absorption and particle size distribution

The bulk density of the biochar was determined by measuring the mass of particles occupying an uncompacted volume (Fig. 3c), which provides an indication of its pore structure and interparticle voids. For this purpose, a container of known volume was gently filled with biochar without applying any compaction, and its mass was recorded. To improve reliability, six readings were taken, and the average bulk density was found to be **0.75 g/cm^3**. The specific gravity of the biochar was measured using a Le-Chatelier flask, and the obtained value was **0.83**. The water absorption capacity of biochar was evaluated using the tea-bag method[43], with three trials

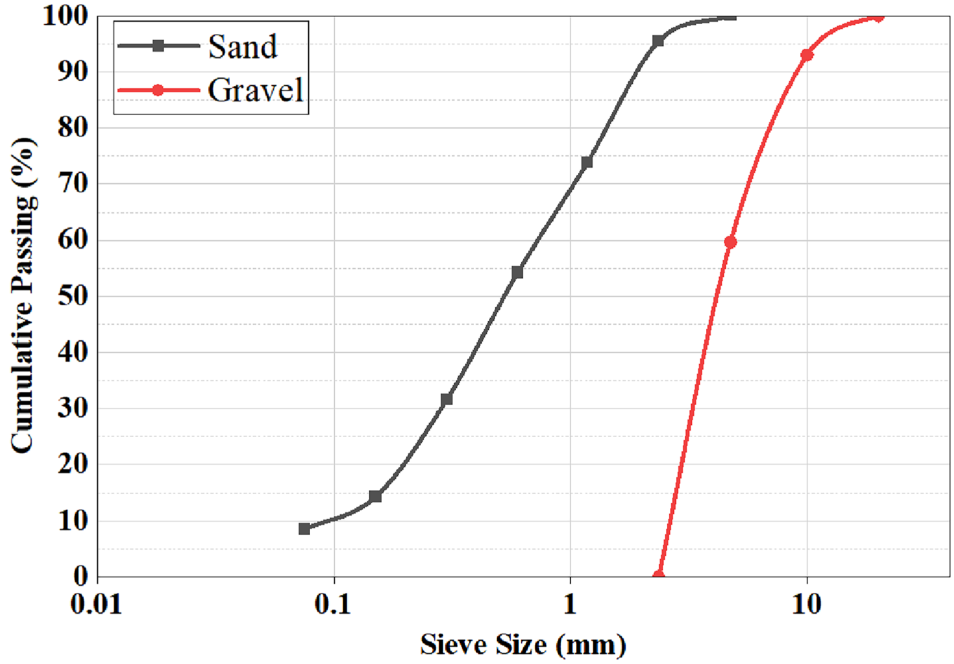

Fig. 2. Particle size distribution curve for fine and coarse aggregate.

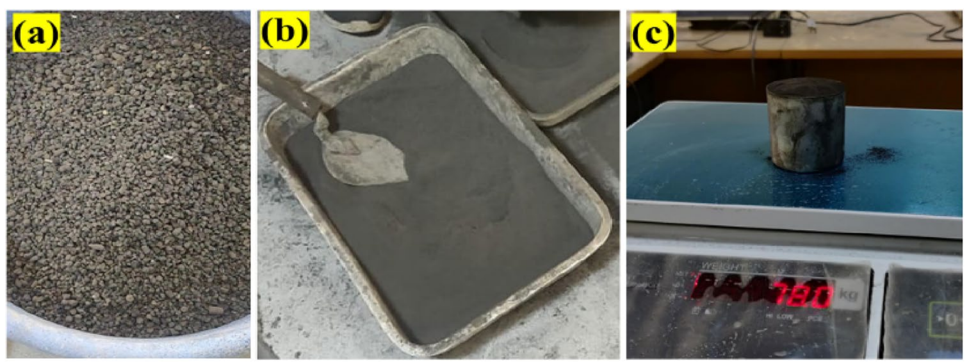

Fig. 3 (**a**) Raw biochar received from site; (**b**) processed biochar after grinding and sieving; (**c**) bulk density measurement of biochar.

conducted to ensure accuracy. Care was taken to properly seal the tea bags to prevent any leakage of biochar. An empty tea bag was used as a reference in the calculation. Each tea bag was filled with biochar and immersed in water under fully saturated conditions for 24 hours. The samples were weighed under saturated surface-dry (SSD) conditions, followed by oven drying to determine the dry weight. Water absorption was calculated as the ratio of the difference between saturated and dry weights to the dry weight of the biochar. The average water absorption capacity of the three specimens was found to be 61%.

Particle size and density distribution curves of the biochar particles used is presented in Fig. 4. The particle size distribution curve is broad with particles of grain sizes for D10, D50, and D90 as 6.4µm, 50.1µm, and 140.8µm, respectively. The detailed analysis of the grain size of biochar is tabulated in Table 3 below.

Microstructure analysis

To explore the suitability of material a detailed microstructure study plan (Fig. 5) was carried out.

Morphology of biochar particles and surface pores was studied using scanning electron microscopy (SEM), performed on JSM-7610FPlus FESEM coupled with an EDX detector to examine the microstructure of biochar as seen in Fig. 6 The low-magnification image (Fig. 6(a)) reveals an irregular, heterogeneous surface morphology

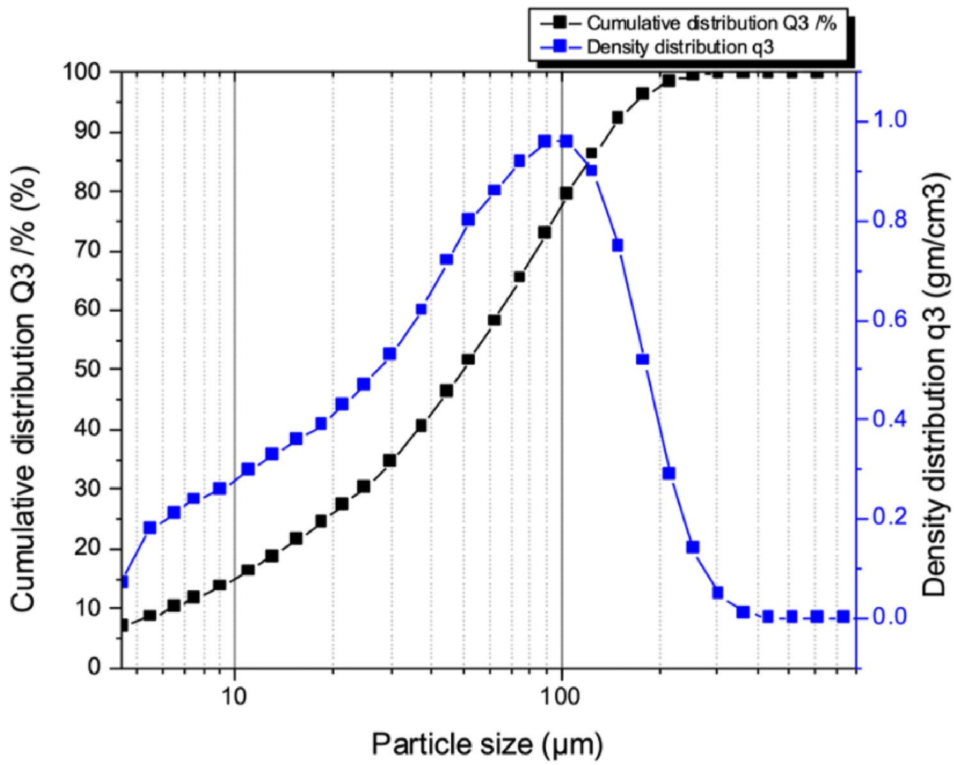

Fig. 4 Particle size distribution curve of biochar post mechanical grinding

Table 3 Analysis of biochar grain (µm).

D10	D16	D50	D84	D90	D99	SMD	VMD	$S_V(m^2/cm^3)$	$S_m(cm^2/g)$
6.4	10.7	50.1	118.4	140.8	233.8	16.54	63.68	0.36	1338.95

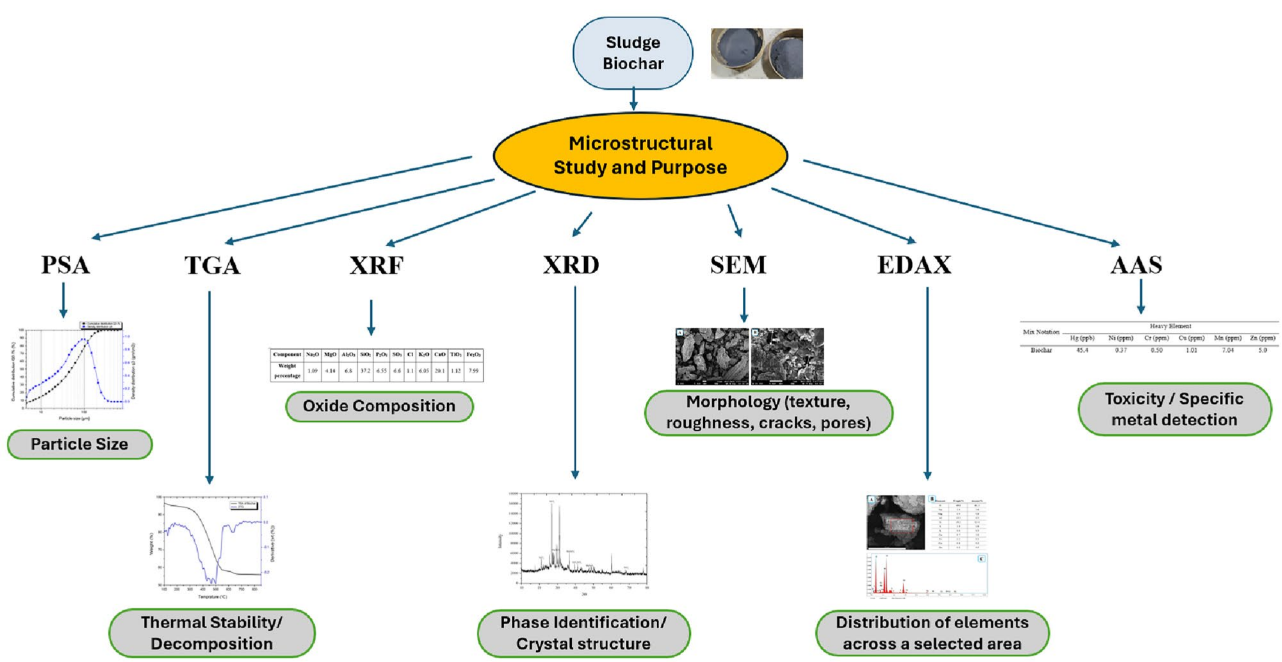

Fig. 5 Microstructural analysis performed and their purpose.

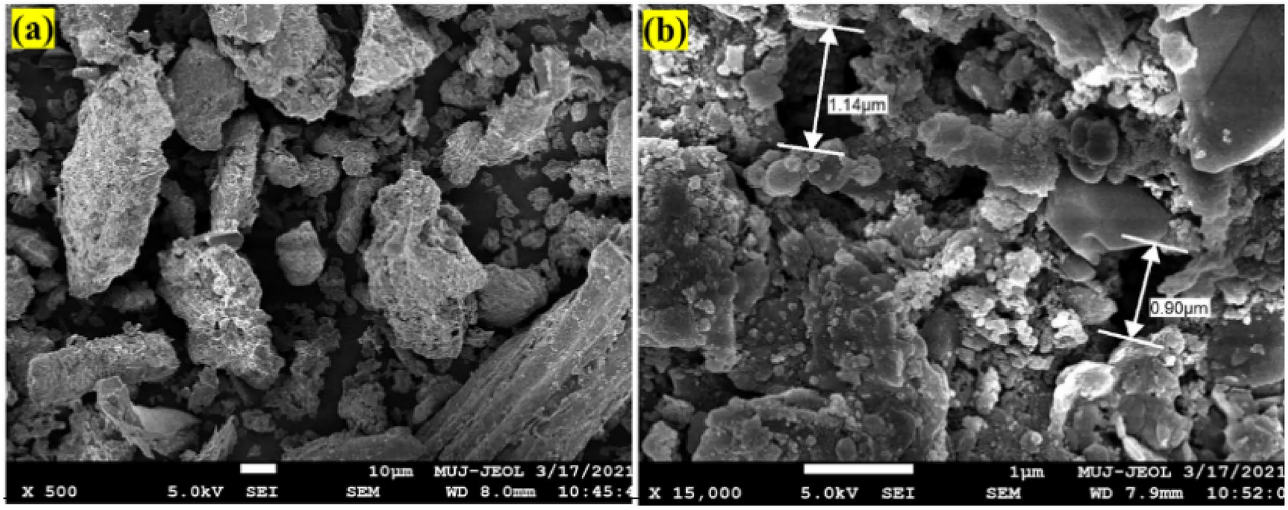

Fig. 6 (**a**) SEM micrograph of biochar particles; (**b**) image showing porous microstructure and its size at 15000x.

Table 4 XRF analysis of biochar.

Component	Na_2O	MgO	Al_2O_3	SiO_2	P_2O_5	SO_3	Cl	K_2O	CaO	TiO_2	Fe_2O_3
Weight percentage	1.09	4.14	6.8	37.2	6.55	6.6	1.1	6.05	20.1	1.12	7.99

characterized by angular and fragmented particles. The structure appears highly rough with loosely packed agglomerates, indicating the presence of significant interparticle voids. At higher magnification (Fig. 6(b)), the biochar exhibits a well-developed porous structure with numerous micro-pores and cavities distributed across the surface. The pore sizes are observed in the micrometer range (approximately 1–10 µm), confirming the highly porous nature of the material. These pores are likely formed due to the release of volatile compounds during the pyrolysis process.

The presence of such a porous and rough surface texture suggests a high surface area, which can enhance water absorption capacity and provide internal curing effects when incorporated into concrete. Additionally, the irregular morphology may contribute to improved mechanical interlocking within the cement matrix.

Overall, the SEM observations confirm that the sludge-derived biochar possesses a highly porous and heterogeneous structure, making it suitable as a lightweight filler material in cementitious composites. The microstructure of biochar particles was found to have, an ability to retain and absorb more water compared to cement and fine aggregate[55,56].

Elemental, crystallinity, and Thermogravimetric analysis

X-ray Fluorescence (XRF) spectroscopy was used to investigate the elemental composition of biochar using a Rigaku Primus-III WD XRF machine. Major compounds identified in the XRF analysis are tabulated in Table 4 below.

The combined content of oxides (SiO_2 + Al_2O_3 + Fe_2O_3) meets the ASTM C618[57] requirement of $\geq 50\%$, as calculated: $37.2 + 6.8 + 7.99 = 51.99\%$. Additionally, Class C fly ash typically contains a high amount of Calcium Oxide (CaO), generally exceeding 20%, which also a criteria fulfilled. Silicon dioxide and calcium oxide are the two major oxides available in biochar to play a key role in binding cement with biochar. For chemical elemental analysis, Energy Dispersive X-ray spectroscopy (EDAX) was performed subsequently with SEM as shown in Fig. 5. The JSM-7610F chamber fitted to the EDAX Energy Dispersive X-ray (EDS) detector has been used for elemental analysis at the micro-nanoscale. The output consists of spectra (Fig. 7b) showing peaks corresponding

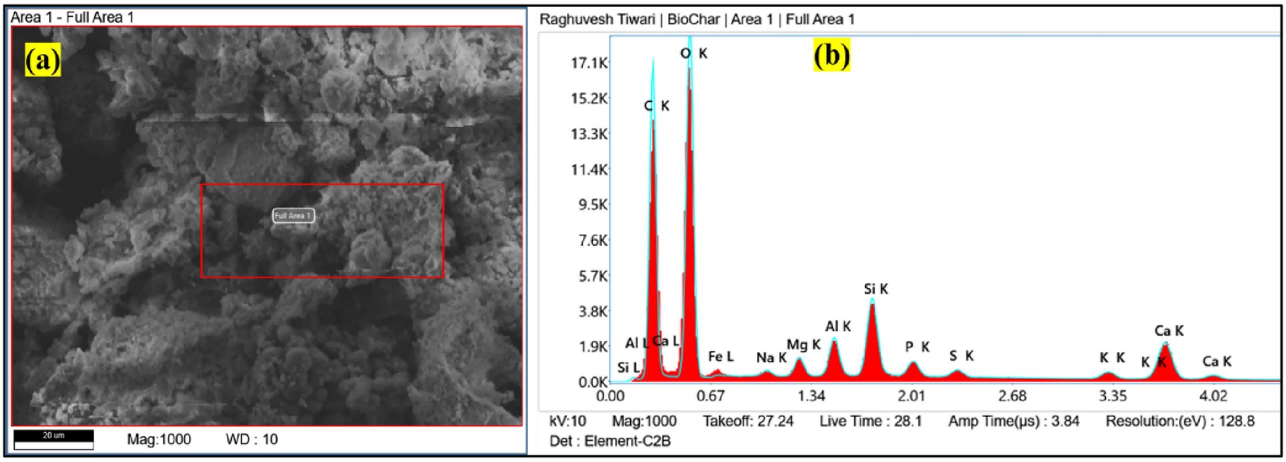

Fig. 7 (**a**) EDAX picture showing area selected of sludge biochar; (**b**) EDAX Spectra showing elemental intensities.

Table 5 Element present in selected region of EDAX.

Element	C	O	Na	Mg	Al	Si	S	K	Ca	Fe	P
Atomic%	61	31.4	0.2	0.4	1.5	1.8	0.2	0.4	2.7	0.6	0.4

to the elements making up the true composition of the sample being analysed. Results of EDAX performed in the marked region of the SEM image (Fig. 7a) show the presence of various elements (Table 5) in biochar, such as O (gaseous chemical element), Carbon, Silica, Aluminium, Calcium, etc.

Crystallinity analysis was performed using X-Ray diffraction spectroscopy (XRD) to carry out the analysis of inorganic pigments and extenders by analysing the crystalline structure of the sample. The test was performed on Rigaku make automated multipurpose X-ray Diffractometer. Biochar was crushed and sieved through 75 um sieve (#200) and the X-rays were then diffracted employing Cu-Ka radiation. Scanning ranges from 10°-80° keeping scan speed 10.00 °/min at Step width of 0.02° was adopted in the test. Peaks of Silica in form of quartz have been observed in the XRD analysis of biochar sample. The presence of same has been confirmed from XRF analysis too. Fig. 8. shows the XRD plot of biochar particles.

To the evaluate the quantity of carbon content in biochar, thermogravimetric analysis was performed on the sample using Shimadzu DTH-60H at a constant temperature change rate of 10°C per minute up to 950°C. The percentage weight loss below 100°C as shown in Fig. 9 is due to moisture removal from biochar and from the temperature range of 350^0C to 500^0C, the weight loss was due to combustion of graphitic carbon fraction[58]. Loss on Ignition for biochar was found to be around 40%.

Hazardous heavy metals in biochar

To know for the concentration of various hazardous heavy metals in biochar concrete, atomic absorption spectroscopy (AAS) was performed. All the specimens were digested in acid mixture of HNO_3 (65%, v/v), HCl (30%, v/v), and HF (40%, v/v) using a Teflon vessel in sealed packed condition and loss of volatile elements were prevented. Sample were espoused for light of different bulbs such as Hg, Zn, Mn, Cu, Ni, and Mn, utilizing their corresponding wavelengths. The instrument was calibrated for each targeted heavy metal using standard solutions of varying concentrations, and calibration curves were developed by plotting absorbance against concentration. The linearity of each curve was verified using the correlation coefficient. Instrument performance was further validated through the use of blanks, replicate measurements, and quality control standards to ensure accuracy and reproducibility.

 https://doi.org/10.1038/s41598-026-66956-6

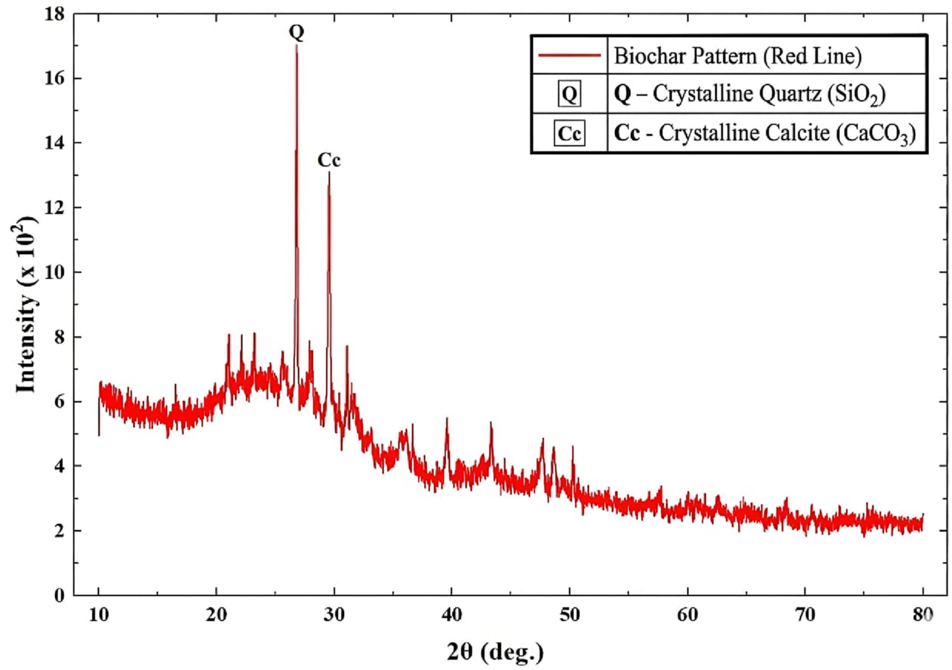

Fig. 8 XRD plot of biochar with presence of SiO_2.

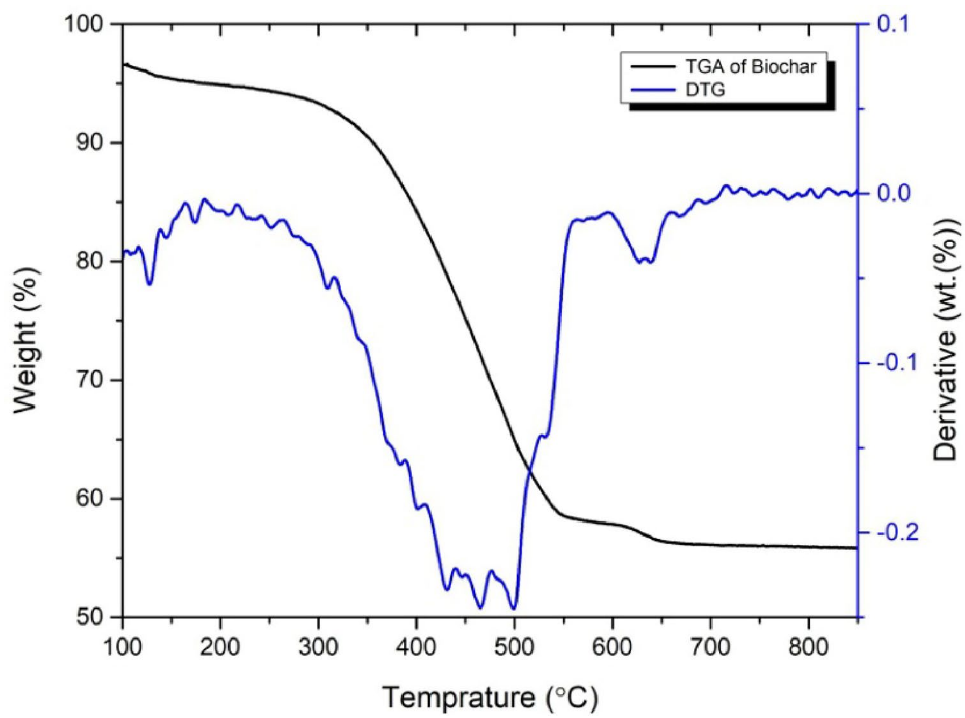

Fig. 9 TGA/DTG curve of sludge biochar.

Micro-raman spectroscopy

The resulting Raman spectra for sample displayed a prominent vibrational modes characteristic of carbonaceous materials (Fig. 10), the defect band (D-band) located at approximately 1350 cm^{-1} and the graphitic band (G-band) located at approximately 1580 cm^{-1}. Biochar exhibited a pronounced graphitic G-band (~1580 cm^{-1}) relative to the defect-induced D-band (~1350 cm^{-1}), with an ID/IG ratio <1, indicating a higher degree of structural ordering and graphitic character.

The presence of sp^2 carbon bonds suggests that there is a large amount of graphitization and heat treatment in the biochar material. As far as its use in concrete production, such a crystalline structure is a good advantage. This means that the biochar material will be resistant to chemical reactions in an extremely alkaline cement hydration medium.

Design mix proportions

A reference cement concrete mix with water binder ratios of 0.40, 0.45, 0.50, 0.55, and 0.60 had been initially prepared in accordance with IS 10262[59]. In the subsequent mixes, biochar at 0, 5, 10, and 15% by weight of cement had been used to replace the cement as a binder in the concrete. The details of the mix designs adopted in the study for evaluation of mechanical strength and durability properties of concrete are in Table 6 along with the slump values of fresh concrete. Sulphonated Naphthalene Formaldehyde in percentage dosage by weight of the binder (0.5%, 1%, 1.5%, and 2%) has been used in the study to maintain adequate workability in the concrete.

The values of slump for mixes with biochar reduced with the increase in dosage of biochar, indicating a drop in workability. This can be attributed to the negative charges produced by the biochar's carboxyl functional groups and absorption capacity of biochar particles. This absorption created a dearth of free water, leading to flocculation and increased interaction between cement particles[60].

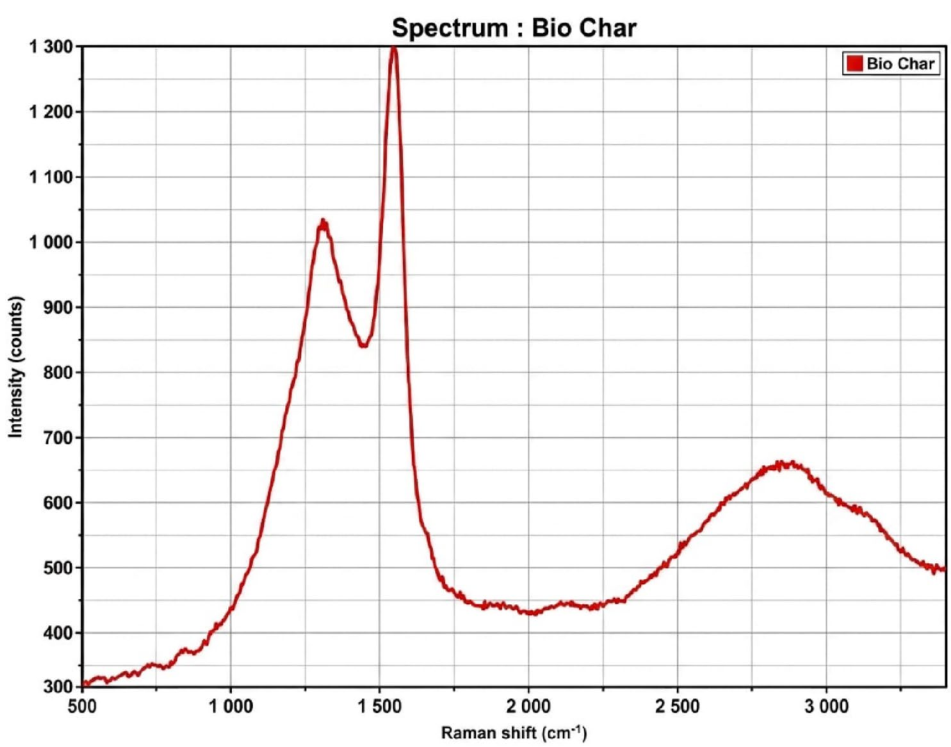

Fig. 10 Raman spectral analysis of graphitic and disordered carbon in biochar.

Table 6 Design mix proportions of Biochar concrete (kg/m^3).

Mix Notation	Water binder ratio	Cement (kg)	Biochar (kg)	Fine aggregate (kg)	Coarse aggregate (kg)	Water (Lit.)	Superplasticizer (kg)	Workability (Slump (mm))
OPC400	0.40	450	0	634	1140	180	4.5	100
BC401		428	23	634	1140	180	6.75	60
BC402		405	45	634	1140	180	6.75	40
BC403		383	68	634	1140	180	9.0	25
OPC450	0.45	400	0	667	1149	180	4.5	120
BC451		380	20	667	1149	180	6.75	80
BC452		360	40	667	1149	180	6.75	65
BC453		340	60	667	1149	180	9.0	45
OPC500	0.50	360	0	698	1152	180	4.5	135
BC501		342	18	698	1152	180	6.75	90
BC502		324	36	698	1152	180	6.75	75
BC503		306	54	698	1152	180	9.0	50
OPC550	0.55	327	0	727	1150	180	2.25	110
BC551		311	16	727	1150	180	6.75	110
BC552		295	33	727	1150	180	6.75	90
BC553		278	49	727	1150	180	9.0	75
OPC600	0.60	300	0	755	1145	180	2.25	110
BC601		285	15	755	1145	180	6.75	115
BC602		270	30	755	1145	180	6.75	105
BC603		255	45	755	1145	180	9.0	100

Methodology and specimen preparation

To evaluate the pozzolanic activity of biochar as a potential partial replacement of cement, Strength activity index with Portland cement had been conducted as per methodology specified in ASTMC311[61]. Although the code specifies to test a 20% replacement of cement with biochar to evaluate strength activity when cured in saturated lime solution, the present study used 5%,10%, 15% and 20% dosages of biochar as partial replacements of cement to study the performance of each dosage. The strength activity has been calculated at 7, 28 and 56 days. 56-day activity was included in the study as the water retention and release capacity of biochar has been reported to extend till 56 days of curing. Drying shrinkage of mortar samples with water binder ratio of 0.50 for 0%, 5%, 10% and 15% dosages have been performed, to study the change in length and shrinkage of the said mixes as per ASTMC311[61]. Preparation of all the specimens were according to ASTM C157/C 157M[62]. The ratio of sand to binder was maintained at 2.5. The change in length of samples of size 25mm × 25mm × 285mm and the values of shrinkage had been measured for 7, 14, 28, 56, 91 and 150 days. While mounting all the specimens on the assembly, free rotation was ensured to avoid any inaccuracies in the results. Design mix proportions for concrete specimens presented in Table 6, cured in water for a period of 28 days, 56 days and 91 days to evaluate the performance of biochar concrete in terms of mechanical strength and durability properties. Mechanical properties such as strength in direct compression and strength in flexure of the water cured sample had been calculated. The samples after curing had been wiped with cloth and dried for 30 min prior to testing.

Compressive strength of the concrete samples was evaluated (Fig. 11D) from concrete cylinders of 150 mm diameter and 300 mm height as per specifications mentioned in IS:516[63] with a loading rate to correspond a stress rate of 140 kg/cm^2/min until failure. In order to evaluate the concrete behaviour in flexure (Fig. 12C), usually measured in terms of modulus of rupture, concrete beams of 100mm height, 100mm width and 500mm tested for different curing period. The loading rate had been maintained at 180 kg/min as per IS:516[63].

Water absorption test and volume of permeable voids test had also been performed on the hardened biochar concrete and compared with reference cement concrete to evaluate the durability of biochar concrete using concrete cubes of 100mm. After curing, the samples were placed in an oven set to 110°C for 24 hours before

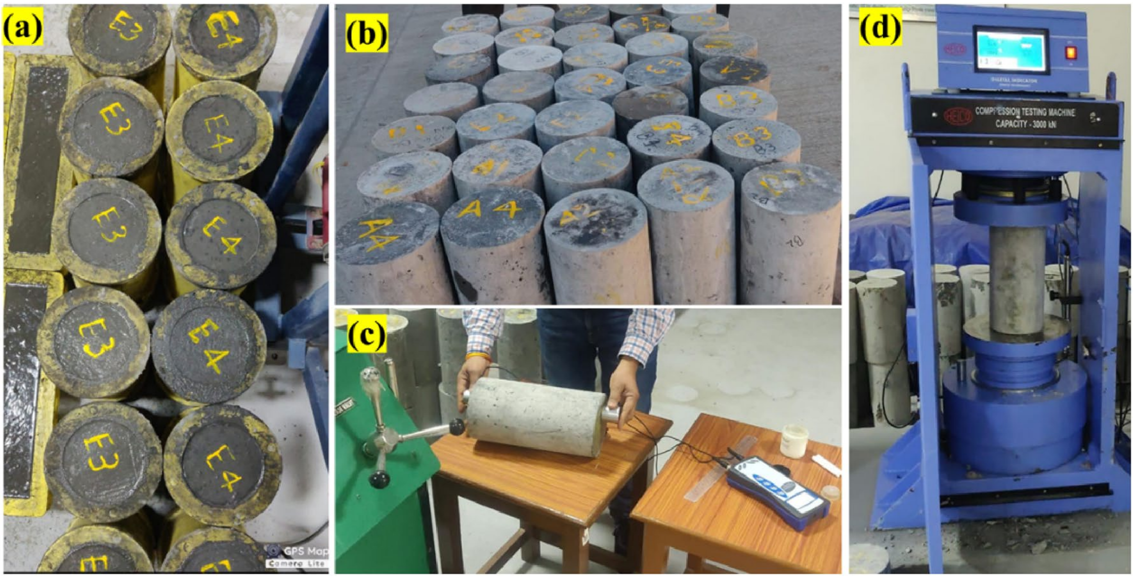

Fig. 11 (**a**) Cylindrical specimen prepared with biochar concrete; (**b**) specimens are ready to test after curing; (**c**) ultra sonic pulse velocity test measurement; (d) compressive strength test on computerised CTM.

Fig. 12 (**a**) Beam specimens prepared; (**b**) specimens just after demoulding; (**c**) three-point load bending test was performed on UTM; (**d**) failure pattern of various specimen.

being submerged in water for 48 hours. The weight gain in the sample is recorded as water absorption of the concrete sample. Following immersion, the samples were rigorously boiled for five hours, surface-dried, and weighed after 14 hours in line with ASTM C642[64]. Following that, each specimen's apparent weight in water was noted, finally giving porosity values in terms of volume of permeable voids. To establish a relationship between the mechanical performance of hardened biochar concrete samples in compression with rebound number, non-destructive test, rebound hammer had been performed on all the concrete samples prior to destructive tests on the samples, cylindrical specimens were tested for surface hardness using a rebound hammer in accordance with

 https://doi.org/10.1038/s41598-026-66956-6

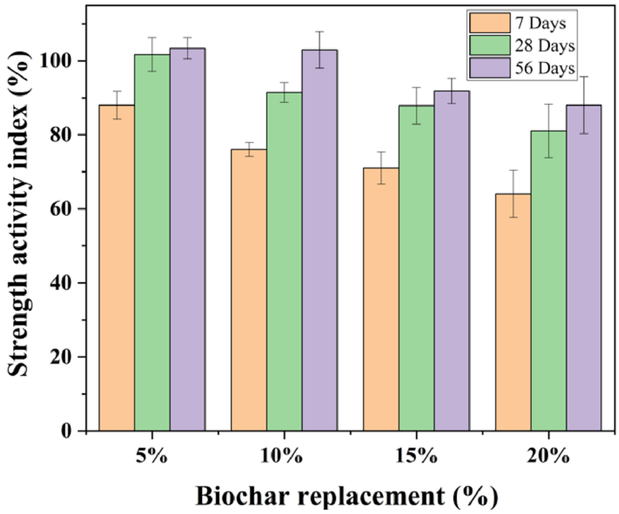

Fig. 13 Strength activity index of biochar mortar.

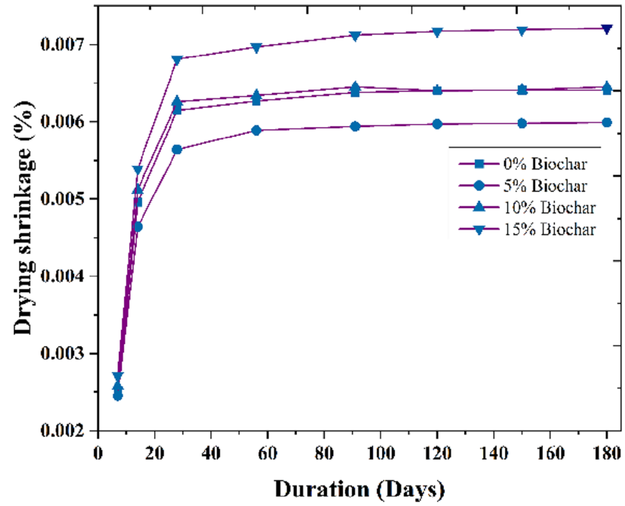

Fig. 14 Drying shrinkage of biochar mortar samples.

IS 13311 (Part 2)[65]. For each cylinder, approximately ten readings were taken, carefully avoiding edges, visible cracks, and honeycombed areas.

Results and discussions

Strength activity index

Strength activity index for various dosages of biochar with Portland cement is represented in Fig. 13. For all dosages of biochar, we have seen a rise in strength activity as the curing time has increased[34]. However, only the mix with 5% biochar showed strength activity of more than 80% in the 7-day curing regime. After 28 days of curing, all biochar dosages displayed increased strength activity of more than 80%, and satisfies the requirements of a materials to be pozzolanic by achieving 75% of strength even with a 20% replacement. Although the 10% biochar concrete displayed low initial strength gain at 7 and 28 days compared to 5% biochar, a similar kind of outcome was also observed by Mensah et. al.[66]. At 56 days, it displayed strength almost similar to the 5% biochar sample. The increase in the strength with curing duration is due to the honeycomb-like pore structure of biochar, making it an excellent water absorbent material that can sustain water and redistribute it to enable internal curing[32,67]. This biochar cement concrete composite acts as a water reservoir, providing a perpetual supply of water internally and increasing the degree of hydration[68] due to significant levels of silica in biochar that bind with the calcium hydroxide to form stable calcium silicates [69]. The increase in the strength activity can also be attributed to the filler effect of biochar particles and reduction in free water, resulting in the increased cohesiveness of the mix.

Drying shrinkage of biochar mortar

The plot of drying shrinkage of biochar cement mortar in Fig. 14 shows that the mix with 5% biochar has lower drying shrinkage compared to the Ordinary Portland Cement (OPC) mortar (0% biochar). A water binder ratio of 0.42 is generally sufficient for complete hydration of cement in sealed conditions[70]. The excess water, which is usually stored in the capillary pores, in the present samples is retained in biochar during initial mixing, leading to a lower binder ratio of the mix, thereby reducing the capillary porosity in the initial curing duration[41].

Hence, in all the mixes adopted in the present study, the maximum shrinkage rate was observed in the first 14 days of curing. The water is slowly released, leading to internal curing and pore refinement, and reduced shrinkage. Hence, although initially the mortar mix with 10% biochar showed higher drying shrinkage compared to OPC mortar, the trend eventually slowed down after a curing duration of 120 days. After 120 days, the drying shrinkage of the 10% biochar mix and the OPC mix had approximately the same values.15% biochar mix displayed higher drying shrinkage values compared to the rest of the mixes, due to increased dosage of biochar leading to the higher self-desiccation of the mix, promoting long term pozzolanic activity, providing ample space for hydration products formation.

Mechanical strength in compression and flexure

Mix notations BC401, BC451, BC501, BC551, and BC601 pertain to concrete mixes with biochar replacing cement by 5% weight. These mixes displayed the highest compressive strength (Fig. 15) and flexural strength (Fig. 17) at 28 days, 56 days, and 91 days curing. The increase in the strength due to biochar is attributed to the water retaining capacity of biochar, resulting in a decrease of the effective water binder ratio for the cement matrix[43].

For mixes BC402, BC452, BC502, BC552, and BC602 that pertain to 10% biochar replacement, the compressive strength and the flexural strength values were lower than control mixes with no biochar (OPC400, OPC450, OPC500, OPC550, and OPC600) at a curing duration of 28 days. A progressive increase in compressive strength was observed in specimens containing biochar, unlike the mix with 0% biochar (Fig. 16). Measurement of compressive strength at 28 days is the reference age for concrete to test, long-term strength gain is generally considered insignificant in conventional concrete design. However, biochar concrete demonstrated continuous strength development even at extended durations, such as 56 and 91 days. At 5% biochar replacement in mixes BC401, BC4501, BC501, BC5501, and BC601, strength increased in all cases, with BC401 showing the highest gain of 22%. An average increase of 12% and 21% in compressive strength of 10% biochar mixes after 56 days and 91 days of curing, respectively was noted.

Biochar particle behaves like a barrier to capillary channels because of fineness by obstructing capillary pores while porous and absorptive nature of biochar is supportive to supply the retained water, promoting secondary hydration and responsible for increased the strength values after 28 days[25]. For 5% biochar mixes, the average increase in compressive strength for 56 days and 91 days was 10% and 20%, respectively. The hydration of cement can be accelerated by biochar particles, assisting in the nucleation and growth of hydration products[71]. Also, better interfacial bonding between biochar particles and concrete matrix proves a compatibility and bonding between hydroxyl groups on biochar particles and cement matrix[72]. In concrete mixes with biochar as a 15% replacement of cement (BC403, BC453, BC503, BC553, and BC603), the dilution effect seemed to have played a predominant role in limiting the production of calcium silicate hydrates and thereby decreased the values of strength[25]. In these mixes, due to an increase in the dosage, biochar particles might have imparted certain brittleness to the hardened concrete sample, enabling crack formation and propagation[73] Pore filling ability of the biochar particles and further densifying the cement colloidal matrix, enhanced the flexural strength of mixes with biochar in concrete, as shown in Fig. 17. Mixes with 5% and 10% biochar replacements seemed to have followed a trend similar to that of compressive strength, where 5% biochar dosage yielded the highest flexural strength, similar results were also reported by Sirico et al.[74]. 5% biochar mixes had an average increase of 25% and 36% in flexural strength at 56 days and 91 days curing, respectively.

Mixes with 10% biochar dosages had 29% and 42% increases in flexural strengths at 56 days and 91 days. The percentage increase in compressive strength was greater than in flexural strength, primarily due to the filler effect of biochar particles, which enhanced particle packing, reduced voids, and improved interfacial bonding between

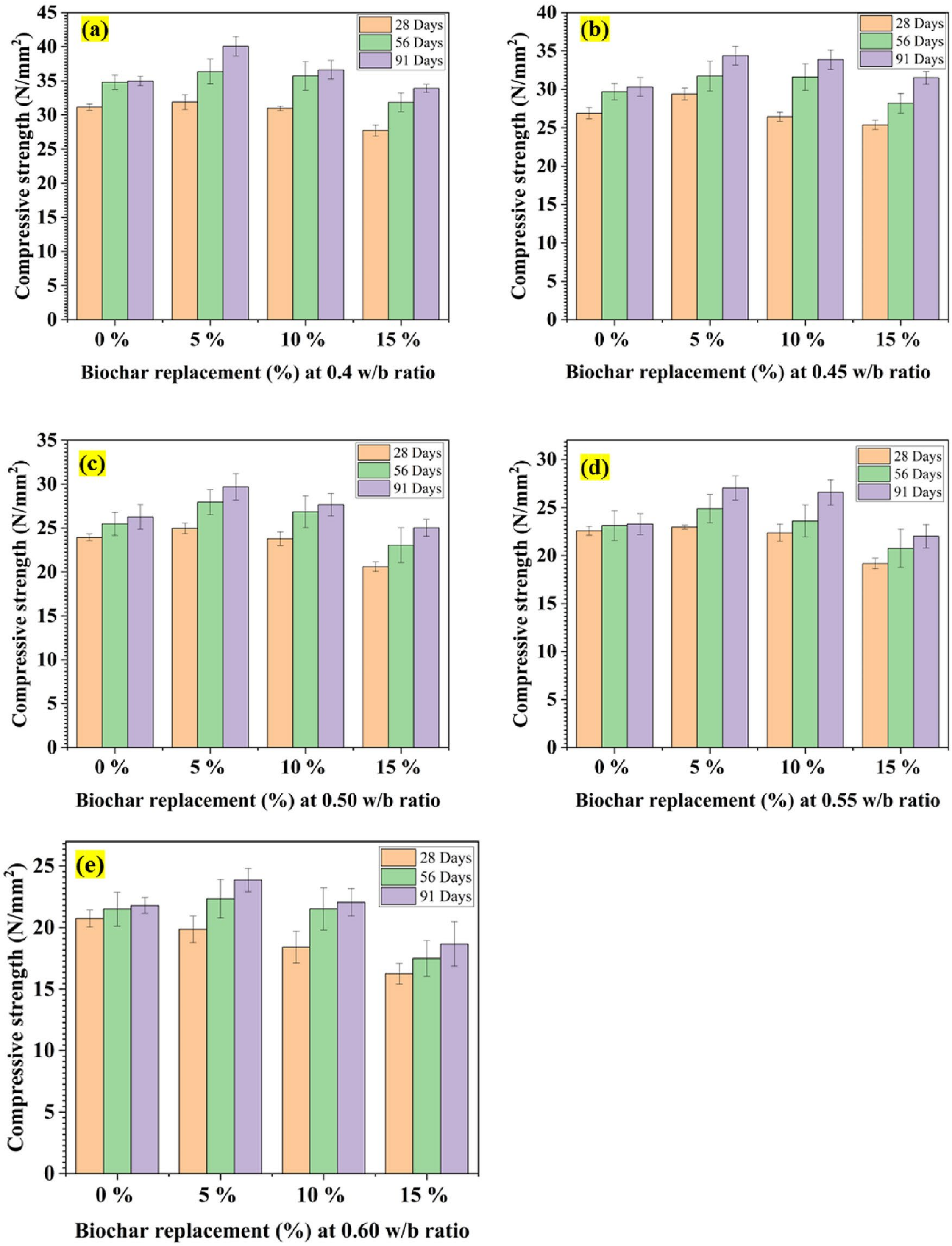

Fig. 15 Compressive strength of concrete mixes with varying biochar dosages and w/b ratio.

the cement paste and aggregates, thereby contributing to better stress redistribution under flexural loading. Fig. 18 illustrates the progressive increase in flexural strength with curing age for the mixes evaluated in this study.

Microstructural characterization using SEM and EDS confirmed the formation of several crystalline phases during cement hydration in the presence of biochar particles. To study all four replacement mixes with a 0.5

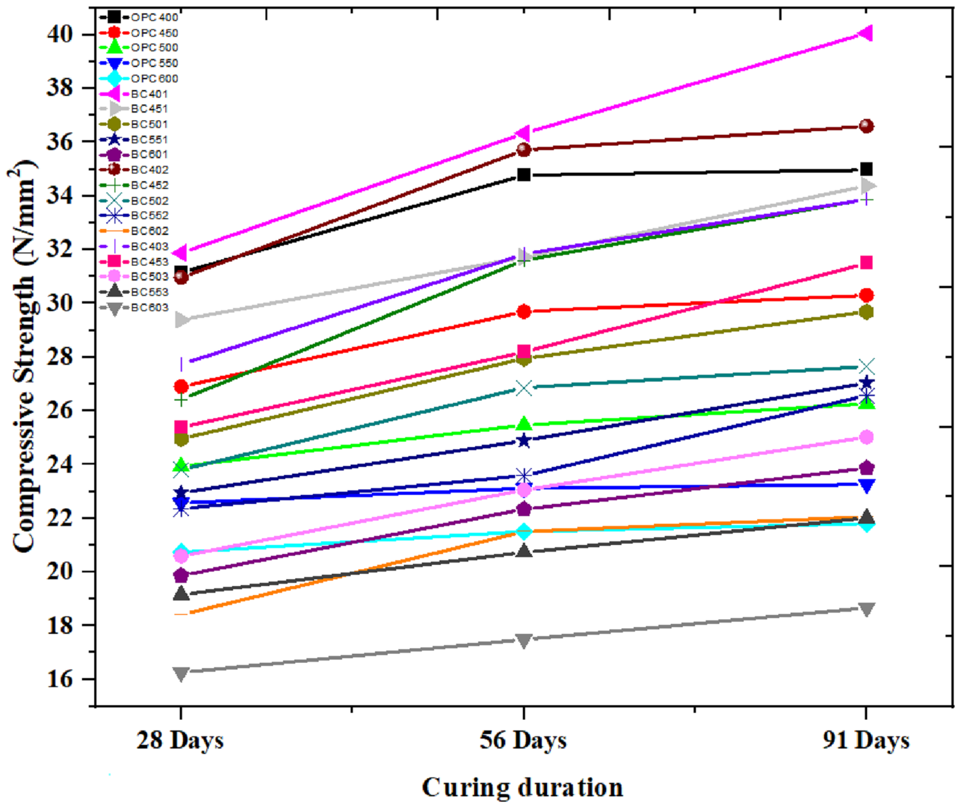

Fig. 16 Compressive strength vs duration.

w/b ratio was preferred. It has been challenging to study biochar cement composites for microstructural properties because of low density and complex porosity[75]. The SEM image and EDS spectrum of plain concrete (Fig. 19) illustrate the elemental composition and the presence of hydration products such as C–S–H, ettringite, and calcium hydroxide (CH). At 5% biochar replacement (Fig. 19b), the SEM micrograph revealed a denser microstructure with a higher amount of C–S–H and portlandite, consistent with the findings of Paula et al.[76]. The EDS analysis showed high carbon content, confirming biochar incorporation, while the presence of Ca and Si indicated the formation of calcium silicate hydrates, essential for strength development. Minor elements such as Mg, Al, and Fe further suggest their participation in pozzolanic reactions[77]. At 10% replacement (Fig. 19c), the microstructure appeared less dense and more porous compared to the 5% mix.

The EDS results revealed a further increase in carbon content and a significant reduction in calcium, confirming dilution of cementitious components. Although a lower Ca/Si ratio is often associated with improved strength[78], our observations showed strength loss at this level, though it remained comparable to the respective control mix. At 15% biochar replacement (Fig. 19d), SEM micrographs exhibited a layered structure with numerous voids and cracks, indicating weak interfacial transition zones and poor particle bonding, which contributed to further strength loss and shows formation of hydration product has been reduced at 15% in Fig. 19d. The corresponding EDS analysis displayed extremely high carbon content and poor C–S–H gel formation. Overall, the microstructural study demonstrated that higher levels of biochar replacement were detrimental to concrete performance.

Regression analysis

To predict the performance of concrete for various biochar replacements at 28, 56 and 91 days, trend lines study were conducted and observed correlation is significant across all water-to-binder ratios at 28 days which is 0.61 for 0.4 w/b ratio and 0.96 for 0.6 w/b ratio in compressive strength and same trend was found in flexural strength as R^2= 0.8212 at 0.4 w/b ratio and R^2=0.8549 at 0.6 w/b, similar kind of study was also demonstrated by Ahmad

 https://doi.org/10.1038/s41598-026-66956-6

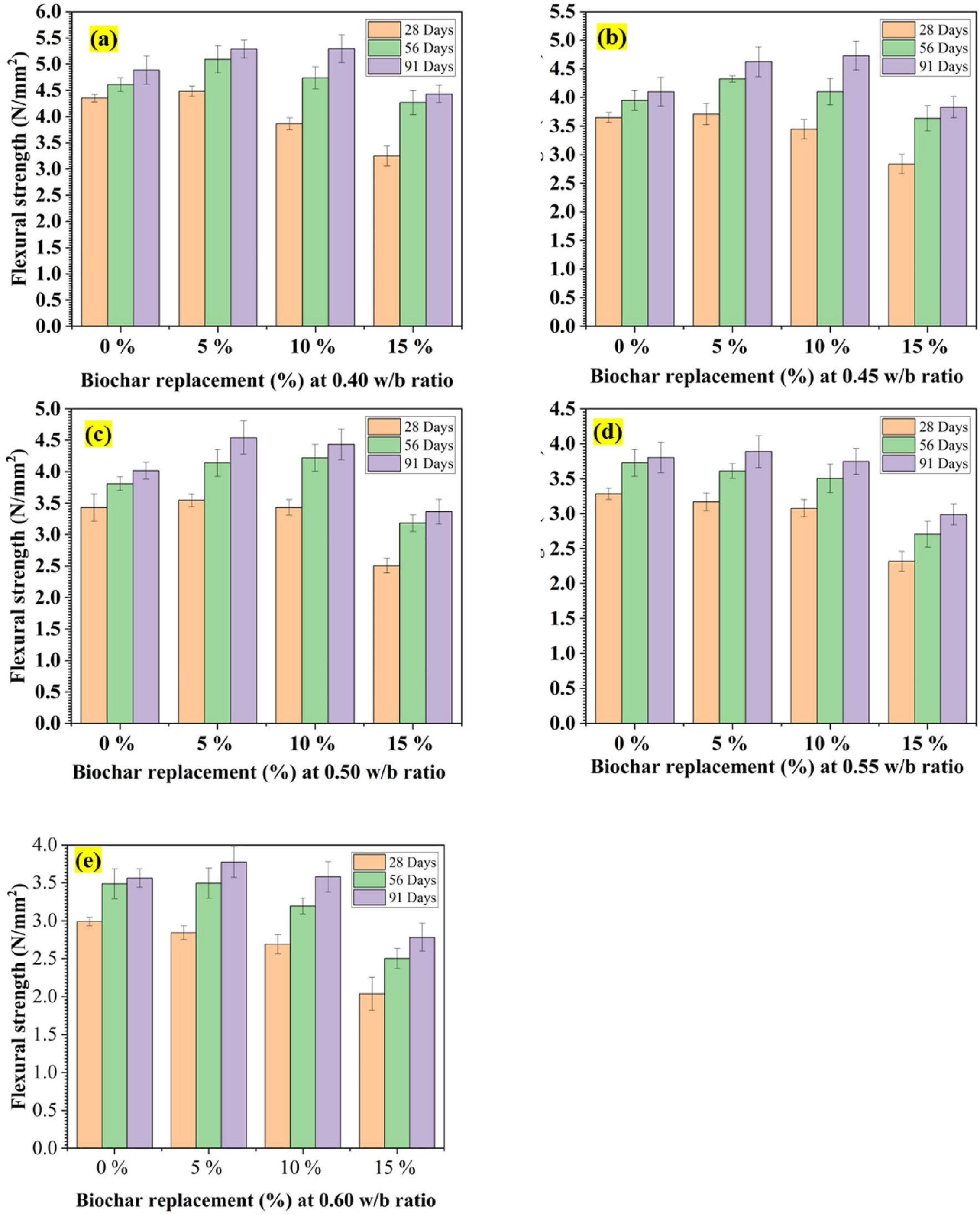

Fig. 17 Flexural strength of concrete mixes with varying biochar dosages and w/b ratio.

et al.,[47]. However, it decreases progressively at 56 days and further at 91 days in most cases. Although higher w/b ratio with higher replacement is giving higher R^2, for w/b ratio 0.6 at 56 days R^2= 0.5796, and at 91 days R^2 =0.4484 in compression and R^2= 0.8123 and R^2= 0.5557 in flexure. This trend suggests that, at early ages, compressive strength is more sensitive to the percentage of biochar replacement, while this effect diminishes over time due to continued hydration and secondary reactions. Notably, a stronger correlation was observed at higher water-to-binder ratios, likely due to the influence of biochar on porosity and microstructural development. All

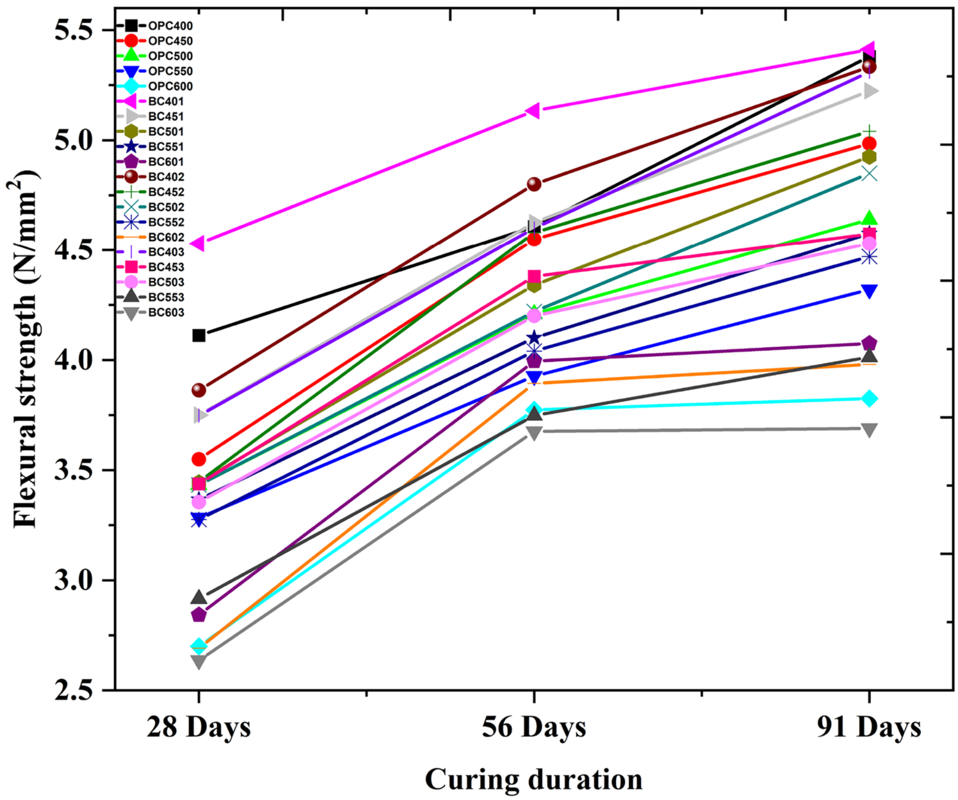

Fig. 18 flexural strength vs duration.

associated data for trendline equations and correlation coefficients are provided in supplementary (*See:* Table S1 & S2).

A study shows that the optimum replacement level for biochar is 5% for enhanced compressive strength, whereas in case of partial replacement of cement with fly ash and rice husk ash in concrete was found that the optimal replacement levels are 30% for fly ash and 7.5% for rice husk ash[79,80]. Rafat and Klaus reported that metakaolin provides optimum strength enhancement at a 20% replacement level[81].

Porosity and water absorption

Plot represents water absorption of the mixes used in the study for various curing durations with respect to replacement of biochar (Fig. 20). Water absorption of the mixes with 5% biochar (BC401, BC451, BC501, BC551, and BC601) was less compared to the control mixes with no biochar for all curing durations. As curing duration increased beyond 28 days, 10% biochar mixes

(BC402, BC452, BC502, BC552, and BC602) also displayed comparable water absorption values to control mixes. Filler effect and internal curing of the biochar particles are responsible for the decrease in the water absorption capacity of mixes with 5% biochar. Sustained release of water and continued hydration and pore refinement are responsible for a perpetual decrease in the water absorption capacity of 10% biochar mixes at long curing durations (>28 days). 15% biochar mixes (BC403, BC453, BC503, BC553, and BC603) showed higher water absorption values, possibly due to the interconnection between macro-pores of biochar with capillary pores of cement matrix at high dosages of biochar, especially in mixes with high water-cement (w/c) ratios[22]. Similar trends have been observed in the measure of porosity in terms of volume of permeable voids as seen in Fig. 21. The incorporation of biochar had refined the porosity of the bulk matrix and interfacial transition zone, leading to lesser porosity. The trend in porosity of biochar concrete samples can also be attributed to the modification of tortuosity and affect the moisture transport phenomena as observed by Gupta et al[32].

 https://doi.org/10.1038/s41598-026-66956-6

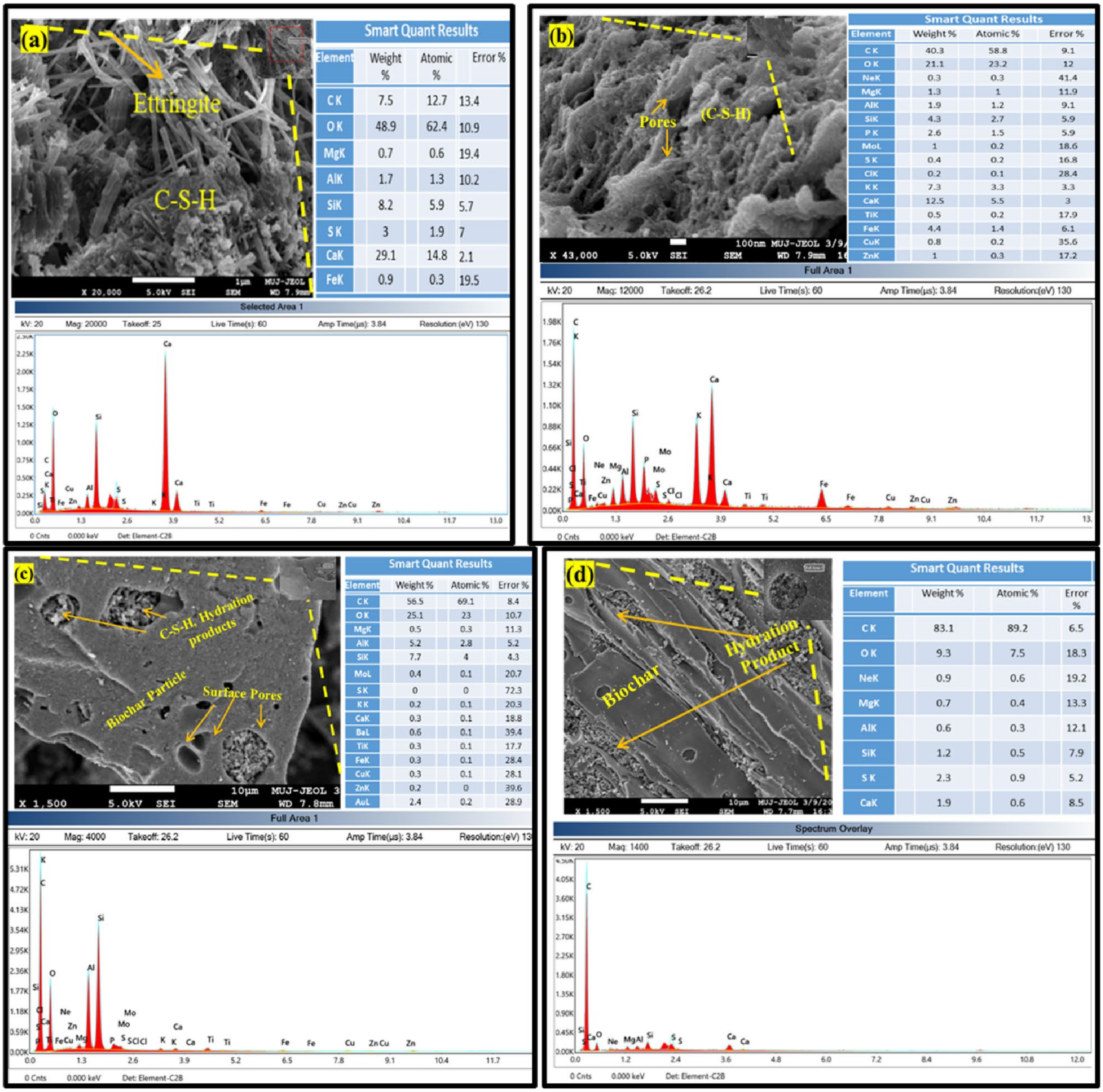

Fig. 19 SEM micrograph including elemental composition and EDAX spectra for 0.5 w/b ratio (**a**) for 0% biochar; (**b**) for 5% biochar; (**c**) for 10% biochar; (**d**) 15% biochar.

FT-Ir analysis

The FT-Ir spectra for Pure Biochar and the four concrete composites with varying biochar content (0%, 5%, 10%, 15%) are displayed in Fig. 22. Analysis of the functional group regions reveals specific compositional variations and interactions within the composite structure.

Detailed examination of the critical bands provides precise value ranges, referencing the experimental dataset: Hydroxide (OH) stretching region (around 3700-3800 cm-1), indicative of hydration, shows peak values precisely at 3733-3737 cm^{-1} (Pure Biochar), 3749 cm1 (0% Concrete), 3743 cm^{-1}, 3737 cm^{-1} (10% Composite), 3737 cm^{-1} (15% Composite) 3735 cm^{-1} (15% Composite). Additional weak bands are present at 3618 cm^{-1} (5%)

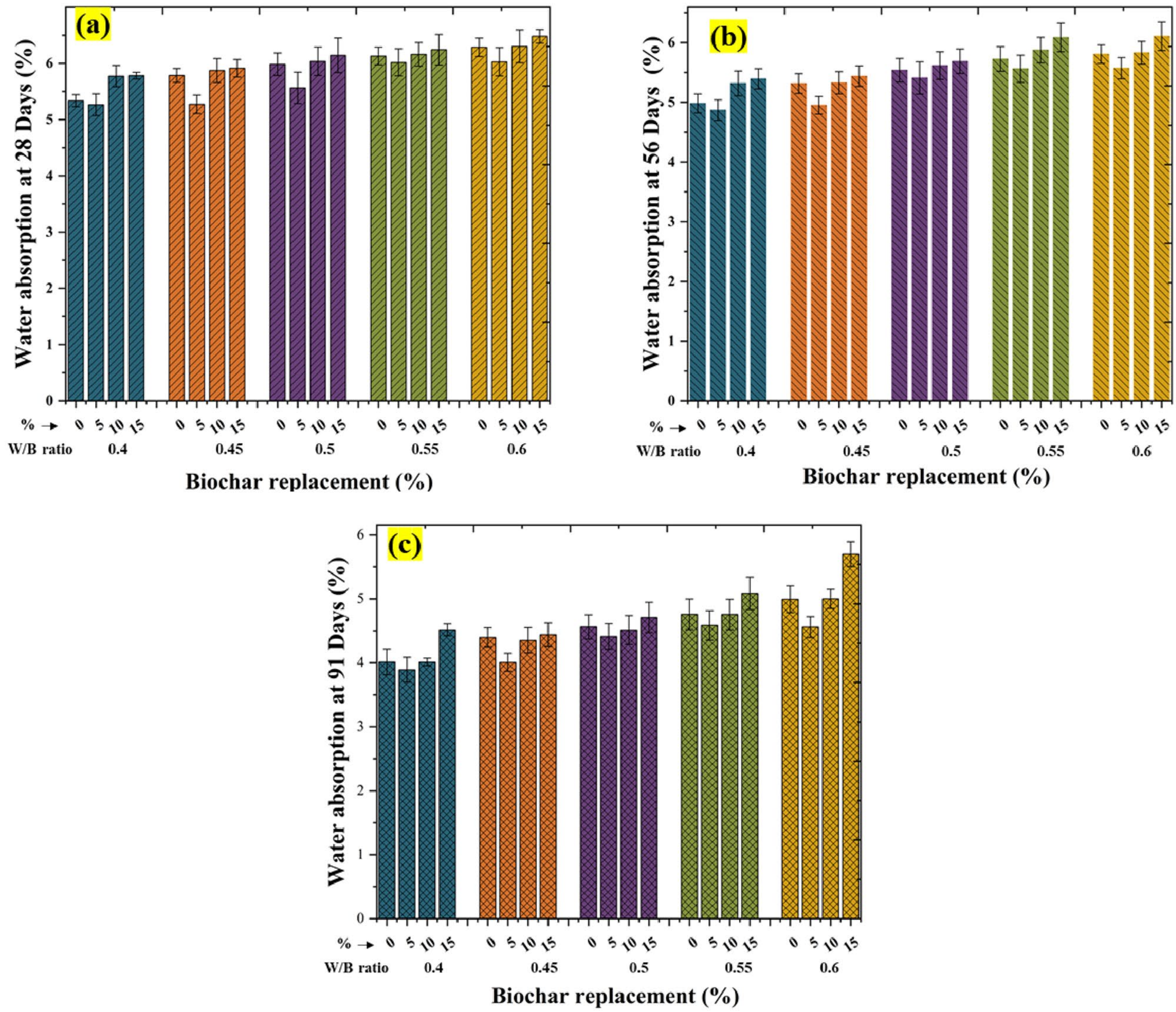

Fig. 20 Average percentage water absorption of concrete mixes with varying biochar dosages (**a**) for 28 days; (**b**) for 56 days; (**c**) for 91 days.

and 3610 cm^{-1} (15%). Carbonate (CO_3) region (prominent around 1500 cm^{-1}), associated with carbon sequestration, has distinct bands at: 1498 cm^{-1} (0%), 1527 cm^{-1} (5%), 1535 cm^{-1} (10%, 1533 cm^{-1} (15%). Pure biochar has a similar, albeit less defined, features. Other associated common carbonate-related bands include around : 785 cm^{-1}, 781 cm^{-1} (5%), 783 cm^{-1} (10%, 783 cm^{-1} (15%). Less prominent bands at around 2320-2350 cm^{-1} (2353 for 1, 2341 for 10%, 2323 for 15%) were recorded. Silicate (Si-O) region (key matrix bands around 1000 cm^{-1}), indicative of concrete matrix integration, as precise bands 1040-1038 cm^{-1} (Pure Biochar, (0%), 966 cm^{-1} (0%), 988 cm^{-1}, 990 cm^{-1}, 1027 cm^{-1} (15%). Other specific bands were noted for 1127 cm^{-1} (0%), 590 cm^{-1} (0%), 1708 cm^{-1} (5%) 50%), 1101 cm^{-1} (5%), 1101 cm^{-1}, 1108 cm^{-1} (10%), 1122 cm^{-1} (15%)[82]. Compositional differences and systematic peak shifts revealed within the composite structures. The strengthening of carbonate band suggests enhanced carbonation and increased CO_2 capture potential. Variations observed across all identified bands confirm the successful integration and interaction between biochar and the concrete matrix, particularly in the high-biochar composite (15%).

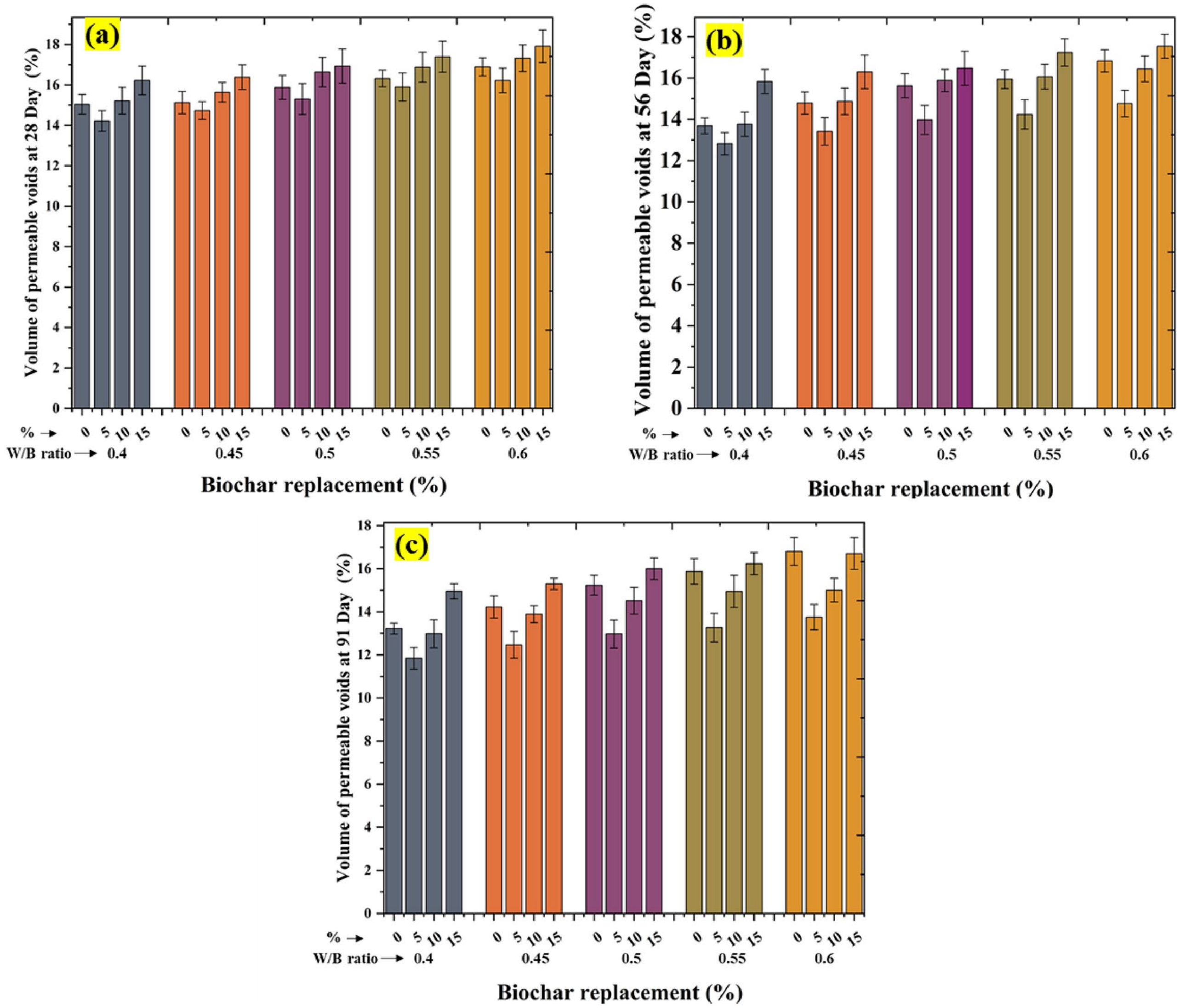

Fig. 21 Average volume of permeable voids of concrete mixes with varying biochar dosages (**a**) for 28 days; (**b**) for 56 days; (**c**) for 91 days.

Relation between rebound number and compressive strength of biochar concrete

To evaluate and develop a relation between rebound number and compressive strength of biochar concrete, concrete cubes of 10mm have been tested in non-destructive testing prior to testing the strength in compression by a destructive method. Most of the literature on the prediction of compressive strength from rebound number is solely focused on rebound number as the only parameter. The prediction expression is usually linear, polynomial, or a power function. No literature on the relation between rebound number and compressive strength has been found for biochar concrete. Hence, in an effort to formulate an expression, porosity in terms of volume of permeable voids had also been adopted as the mechanical performance of biochar had been observed to have been significantly influenced by the porosity of the concrete composite and its water retaining capacity. For the present study, the dosage of biochar has been limited to 15%. Equation 1 shows the expression relating compressive strength to rebound number and porosity. The relationship between rebound hammer and compressive strength of biochar concrete is a polynomial regression of second order using least-squares regression to statistically capture the influence of variables (R and P) on compressive strength (f_c). Below are the indicators used.

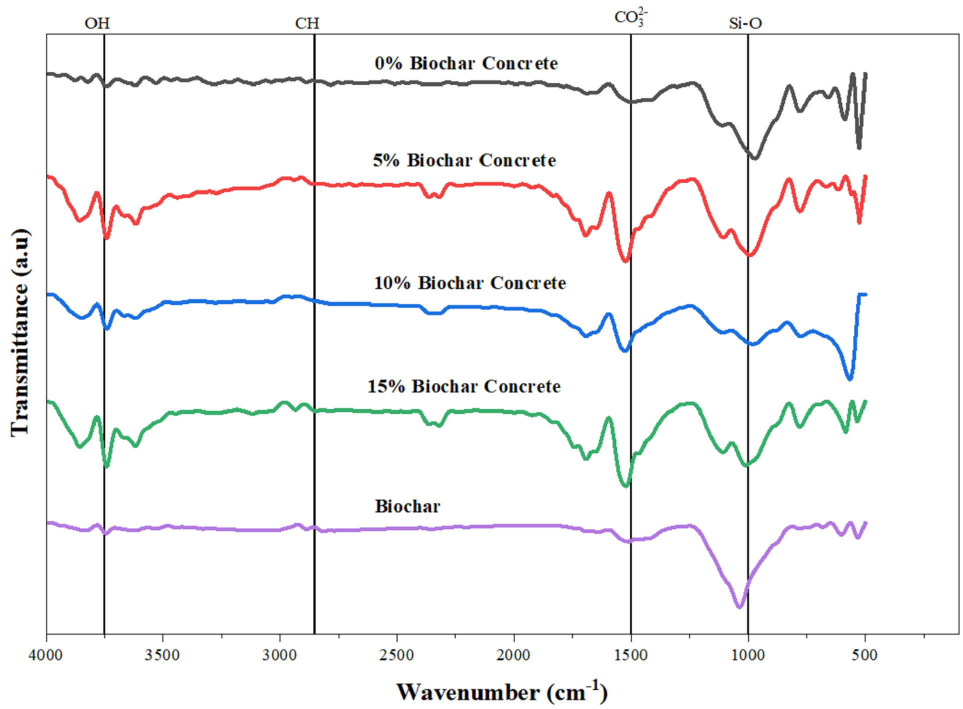

Fig. 22 FT-Ir spectra of pure biochar and biochar concrete composites.

$$R^2 = 0.88265;\ \text{Adjusted}R^2 = 0.87636;\ \text{RMSE} = 12.8385;\ \text{SSE} = 9230.3$$

Fig. 23 shows the plot of Equation 1 representing relationship between rebound number, porosity, and compressive strength.

$$f_c = 210.90 - 8.25R - 9.57P + 0.08R^2 + 0.32PR \quad (1)$$

Where f_c represents the compressive strength
R represents rebound number and
P represents porosity in percentage

Heavy metals detection using Atomic Absorption Spectroscopy (AAS)

Heavy metal detection on samples with different amounts of biochar shows that biochar can trap heavy metals in the cement concrete matrix. The quantity of heavy metals found at different amounts of biochar is shown in Table 7. We chose concrete samples of different biochar dosages with a water binder (w/b) ratio of 0.5 (BC501, BC502, and BC503) to compare to raw biochar particles as they were received. Biochar is an alkaline substance that contains minerals like magnesium, aluminum, and calcium, as well as many anions[83]. These characteristics facilitate the precipitation or immobilization of heavy metals via complexation and enhance the generation of additional gelling products during the hydration reaction[84]. Cement-biochar composites; having OH^- and C-S-H functional groups help remove metals via precipitation, adsorption mechanisms[85]. The amount of heavy metals went down as the amount of biochar in the concrete went up. Because Hg is volatile and sensitive to the environment, samples exhibit more variation at 5%. The other mixtures, on the other hand, followed a steady trend, which could be due to curing and mixing. Chen et al. also said that sludge biochar is useful for keeping heavy metals in concrete[86]. When biochar was utilized in concrete, the levels of Hg, Zn, and Mn dropped significantly. This shows that biochar can trap these metals when used in concrete. Li, Geng, et al. demonstrated the similar findings as cement with biochar shows reduction in leaching fraction, increase in residual (stable) fraction of heavy metals. Helpful for showing how cement with biochar acts to capture metals[87]

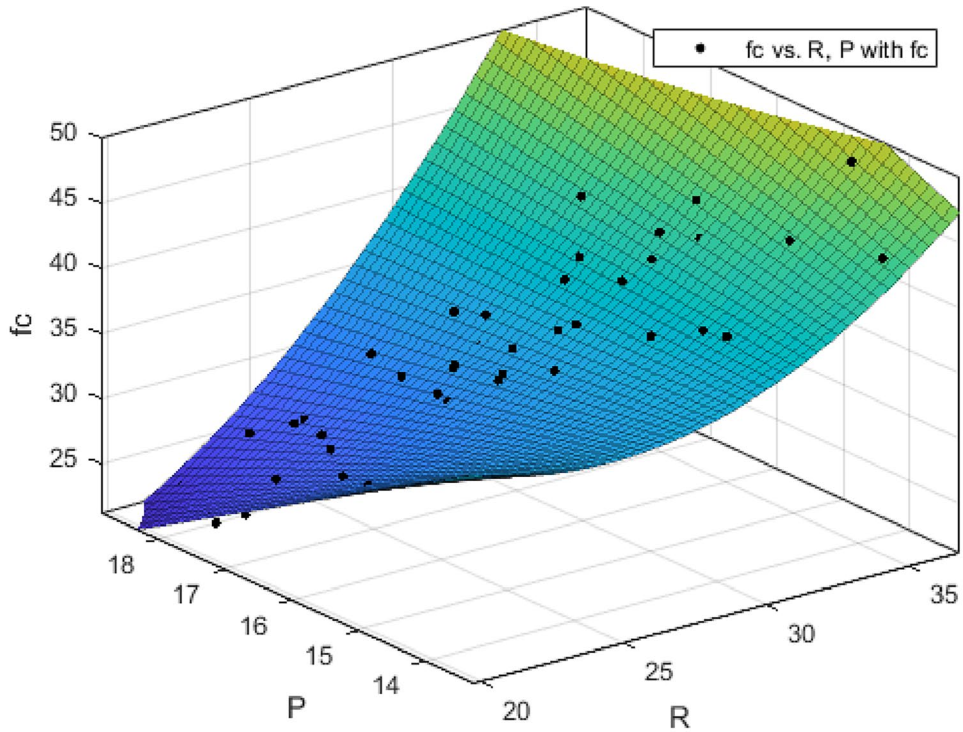

Fig. 23 Plot of rebound number and porosity vs compressive strength.

Table 7 Concentrations of heavy metals in biochar and biochar concrete samples.

Mix Notation	Heavy Element					
	Hg (ppb)	Ni (ppm)	Cr (ppm)	Cu (ppm)	Mn (ppm)	Zn (ppm)
Biochar	45.4	0.37	0.50	1.01	7.04	5.0
BC501	5.09	0.36	0.04	0.25	1.34	0.71
BC502	24.9	0.36	0.12	0.92	1.70	0.80
BC503	35.2	0.36	0.14	0.96	1.67	0.82

Conclusions

The experimental research attempted to examine the suitability of biochar obtained from FSTP by partially replacing cement in concrete. Mechanical and durability properties of biochar concrete with 0, 5, 10, and 15 percentage dosage of biochar, along with water binder ratio ranging from 0.45 to 0.60, have been determined as follows :

- The strength activity of biochar-modified concrete improves with curing age, primarily due to the filler effect of biochar and reduced free water, which enhances mix cohesiveness. Significant early-age drying shrinkage was observed, especially at higher dosages (15%), likely due to self-desiccation and pore structure development.
- Concrete containing 5–10% biochar showed improved compressive and flexural strengths at later ages (56 and 91 days) compared to the control mix, while a higher replacement level (15%) resulted in reduced strength performance.
- Reduced water absorption of concrete at 5 and 10 % biochar has been established through sustained water release and pore refinement, whereas higher water absorption for 15% biochar mixes is the result of the interconnection between macropores of biochar with cement's capillary pores.
- Porosity in terms of volume of permeable voids of biochar concrete exhibits the same pattern as water absorption. Lower porosity was due to the refinement of porosity of the bulk matrix and interfacial transition zone, modification of tortuosity, and effect of the moisture transport phenomena.

- Biochar's increased dosage in concrete has reduced the concentration of heavy metals, indicating the encapsulating ability of biochar. Incorporation of biochar as cement replacement in concrete has comparable mechanical and durability properties, along with reduced concentrations of heavy metals for environmental suitability.

The findings from this investigation indicate that biochar-incorporated concrete can achieve comparable, and in some cases improved, strength characteristics, making it a sustainable alternative to conventional concrete mixes and a viable as a partial replacement for cement in concrete. further evaluation can be extended for long-term durability of sludge biochar-based concrete under various environmental conditions.

Limitations and future scope

While this study provides a foundational understanding of faecal sludge-derived biochar concrete, several limitations remain that offer pathways for future research. As a limitation of the present work, comprehensive durability investigations could not be incorporated within the scope of present manuscript. However, these aspects will be addressed in forthcoming research, where detailed durability evaluations will be carried out and reported. Furthermore, to assess the potential environmental impact associated with the use of sludge biochar, TCLP (Toxicity Characteristic Leaching Procedure) analysis will also be incorporated in future studies to evaluate the leaching behavior of potentially toxic contaminants and to ensure the environmental safety of material. Also, present findings are based on feedstock from a specific subset of Faecal Sludge Treatment Plants (FSTPs); therefore, future studies will incorporate a broader variety of feedstock from diverse geographical regions to validate and generalize these results. Furthermore, while the technology shows promise, the initial capital and operational costs associated with scaling up production may pose challenges in certain developing regions. Future research may also include a comprehensive techno-economic and socio-environmental impact assessment. The current scope was restricted to controlled conditions, and further investigation is required to evaluate the performance of biochar systems under extreme environmental stressors, such as freeze-thaw cycles, high-salinity coastal climates, and extreme temperature fluctuations.

Supplementary Information The online version contains supplementary material available at https://doi.org/10.1038/s41598-026-66956-6.

Acknowledgement The authors wish to thank Manipal University Jaipur for providing the support and infrastructure. The Authors also express their gratitude for the Manipal Research Board (MRB), Manipal Academy of Higher Education and Manipal University Jaipur for supporting the study. The authors thank Tide Technocrats Pvt. Ltd, Telangana, India for their extended support in providing biochar used in the present study. The authors would also like to extend appreciation to SICART, Gujrat and SAIF lab facility & the department of civil engineering at Manipal University Jaipur for all the help rendered in carrying out the research.

Author contributions Raghuvesh Tiwari: Conceptualization; Data curation; Formal analysis; Methodology; Investigation; Visualization; Writing original draft, Review, and editing draft preparation. Priyansha Mehra: Conceptualization; Data curation; Formal analysis; Methodology; Supervision; Investigation; Resource; Validation; Visualization; Writing original draft, Review, and editing draft preparation. Shaik Hussain: Conceptualization; Data curation; Formal analysis; Investigation; Visualization; Writing original draft, Review, and editing draft preparation. Sanchit Anand: Formal analysis; Investigation Methodology; Supervision; Review and editing draft preparation.

Funding Open access funding provided by Manipal University Jaipur. This research did not receive specific grant from funding agencies in the public, commercial, or not-for-profit sectors.

Data availability All the data generated during this study is provided in the manuscript.

Declarations

Competing interests The authors declare no competing interests.

Consent for publication The research has been scientifically consented to be published. Competing Interests The authors declare no competing interests.

References

1. Worrell, E., Price, L., Martin, N., Hendriks, C. & Meida, L. O. Carbon dioxide emissions from the global cement industry. *Annu. Rev. Energy Environ.* **26**(1), 303–329 (2001).
2. Proaño, L., Sarmiento, A. T., Figueredo, M. & Cobo, M. Techno-economic evaluation of indirect carbonation for CO2 emissions capture in cement industry: a system dynamics approach. *J. Clean. Prod.* **263**, 121457 (2020).
3. Geng, Y., Wang, Z., Shen, L. & Zhao, J. Calculating of CO2 emission factors for Chinese cement production based on inorganic carbon and organic carbon. *J. Clean. Prod.* **217**, 503–509 (2019).
4. Olajire, A. A. A review of mineral carbonation technology in sequestration of CO2. *J. Pet. Sci. Eng.* **109**, 364–392 (2013).
5. Xi, F. et al. Substantial global carbon uptake by cement carbonation. *Nat. Geosci.* **9**(12), 880–883 (2016).
6. Mehta, P. K. Greening of the concrete industry for sustainable development. *Concr. Int.* **24**(7), 23–28 (2002).
7. Pavlíková, M. et al. Valorization of wood chips ash as an eco-friendly mineral admixture in mortar mix design. *Waste Manag.* **80**(89), 100 (2018).
8. Ibrahim, S. & Meawad, A. Assessment of waste packaging glass bottles as supplementary cementitious materials. *Constr. Build. Mater.* **182**, 451–458 (2018).
9. Nguyen, T. B. T., Chatchawan, R., Saengsoy, W., Tangtermsirikul, S. & Sugiyama, T. Influences of different types of fly ash and confinement on performances of expansive mortars and concretes. *Constr. Build. Mater.* **209**, 176–186 (2019).
10. Nicula, L. M. et al. The influence of blast furnace slag on cement concrete road by microstructure characterization and assessment of physical-mechanical resistances at 150/480 days. *Materials* **16**(9), 3332 (2023).
11. Waqar, A. et al. Effect of volcanic pumice powder ash on the properties of cement concrete using response surface methodology. *J. Build. Pathol. Rehabilit.* **8**(1), 17 (2023).
12. Zhang, S., Fan, Y., Huang, J. & Shah, S. P. Effect of nano-metakaolinite clay on the performance of cement-based materials at early curing age. *Constr. Build. Mater.* **291**, 123107 (2021).
13. Kashyap, V. S., Sancheti, G. & Yadav, J. S. Durability and microstructural behavior of nano silica-marble dust concrete. *Clean. Mater.* **7**, 100165 (2023).
14. Uddin, M. A. et al. Effect of silica fume on compressive strength and water absorption of the Portland cement–silica fume blended mortar. *Arab. J. Sci. Eng.* **49**(4), 4803–4811 (2024).
15. Olaiya, B. C., Lawan, M. M., Olonade, K. A. & Segun, O. O. An overview of the use and process for enhancing the pozzolanic performance of industrial and agricultural wastes in concrete. *Discov. Appl. Sci.* **7**(3), 164 (2025).
16. Srinivasan, R. & Sathiya, K. Experimental study on bagasse ash in concrete. *Int. J. Serv. Learn. Eng. Humanit. Eng. Soc. Entrep.* **5**(2), 60–66 (2010).
17. Su, Q. & Xu, J. Mechanical properties of rice husk ash and glass powder concrete: Experimental and mesoscopic studies. *J. Build. Eng.* **95**, 110278 (2024).
18. Rathore, Y. & Raheem, J. Synergistic influence of Vindhyan sandstone manufactured sand and rice husk ash on concrete performance. *Natl. Acad. Sci. Lett.* **48**(3), 357–362 (2025).
19. Rathore, Y., & Raheem, J. Experimental investigation of concrete performance incorporating deccan basalt manufactured sand and rice husk ash. *National Academy Science Letters*, 1-9 (2025).
20. Shang, X. et al. Production, properties and life cycle assessment of artificial lightweight aggregates produced with corn straw ash (CSA) and concrete slurry waste (CSW). *Constr. Build. Mater.* **411**, 134274 (2024).
21. Raggiotti, B. B., Positieri, M. J. & Oshiro, Á. Natural zeolite, a pozzolan for structural concrete. *Procedia Struct. Integr.* **11**, 36–43 (2018).

22. Walker, R. O. S. A. N. N. E. & Pavía, S. A. R. A. Physical properties and reactivity of pozzolans, and their influence on the properties of lime–pozzolan pastes. *Mater. Struct.* **44**(6), 1139–1150 (2011).
23. McGrath, M. Climate change: China aims for 'carbon neutrality by 2060'. *bbc News*, *22*. (2020).
24. Sri Shalini, S., Palanivelu, K., Ramachandran, A. & Raghavan, V. Biochar from biomass waste as a renewable carbon material for climate change mitigation in reducing greenhouse gas emissions—A review. *Biomass Convers. Biorefin.* **11**(5), 2247–2267 (2021).
25. Ghani, W. A. W. A. K. et al. Biochar production from waste rubber-wood-sawdust and its potential use in C sequestration: chemical and physical characterization. *Ind. Crops Prod.* **44**, 18–24 (2013).
26. Amalina, F. et al. Biochar production techniques utilizing biomass waste-derived materials and environmental applications–A review. *J. Hazard. Mater. Adv.* **7**, 100134 (2022).
27. Akinyemi, B. A. & Adesina, A. Recent advancements in the use of biochar for cementitious applications: a review. *J. Build. Eng.* **32**, 101705 (2020).
28. Olaiya, B. C., Lawan, M. M., Olonade, K. A. & Abubakar, S. A. Development of sustainable sandcrete bricks using industrial and agricultural waste. *Sci. Rep.* **15**(1), 17202 (2025).
29. Wang, M. et al. Review on utilization of biochar for metal-contaminated soil and sediment remediation. *J. Environ. Sci.* **63**, 156–173 (2018).
30. Smith, P. Soil carbon sequestration and biochar as negative emission technologies. *Glob. Change Biol.* **22**(3), 1315–1324 (2016).
31. Mukherjee, A. & Zimmerman, A. R. Organic carbon and nutrient release from a range of laboratory-produced biochars and biochar–soil mixtures. *Geoderma* **193**, 122–130 (2013).
32. Gupta, S., Kua, H. W. & Low, C. Y. Use of biochar as carbon sequestering additive in cement mortar. *Cement Concr. Compos.* **87**, 110–129 (2018).
33. Sirico, A. et al. Biochar-based cement pastes and mortars with enhanced mechanical properties. *Fract. Struct. Integr.* **14**(54), 297 (2020).
34. Pecha, M. B., Tunstall, L., & Hylton, J. *Biochar as a building material: Sequestering carbon and strengthening concrete* (No. NREL/PR-2800-82445). National Renewable Energy Laboratory (NREL), Golden, CO (United States). (2022).
35. Tan, K. H., Wang, T. Y., Zhou, Z. H. & Qin, Y. H. Biochar as a partial cement replacement material for developing sustainable concrete: An overview. *J. Mater. Civ. Eng.* **33**(12), 03121001 (2021).
36. Ferro, L. R. G. Nanoparticles from food waste: A "green" future for traditional building materials. In *Proceedings of the 9th International Conference on FraMCoS-9, Berkeley, CA, USA* (Vol. 29, pp. 1-6) (2016).
37. Khushnood, R. A. et al. Carbonized nano/microparticles for enhanced mechanical properties and electromagnetic interference shielding of cementitious materials. *Front. Struct. Civ. Eng.* **10**(2), 209–213 (2016).
38. Zhao, S., Huang, B., Shu, X. & Ye, P. Laboratory investigation of biochar-modified asphalt mixture. *Transp. Res. Rec.* **2445**(1), 56–63 (2014).
39. Park, J. H., Lim, K. M., Ryu, G. S., Koh, K. T. & Kim, K. C. An experimental study on the thermal insulation properties of concrete containing wood-based biochar. *Appl. Sci.* **15**(19), 10560 (2025).
40. Praneeth, S., Guo, R., Wang, T., Dubey, B. K. & Sarmah, A. K. Accelerated carbonation of biochar reinforced cement-fly ash composites: enhancing and sequestering CO2 in building materials. *Constr. Build. Mater.* **244**, 118363 (2020).
41. Gupta, S. & Kua, H. W. Carbonaceous micro-filler for cement: effect of particle size and dosage of biochar on fresh and hardened properties of cement mortar. *Sci. Total Environ.* **662**, 952–962 (2019).
42. Gupta, S. & Kua, H. W. Effect of water entrainment by pre-soaked biochar particles on strength and permeability of cement mortar. *Constr. Build. Mater.* **159**, 107–125 (2018).
43. Gupta, S., Kua, H. W. & Dai Pang, S. Biochar-mortar composite: Manufacturing, evaluation of physical properties and economic viability. *Constr. Build. Mater.* **167**, 874–889 (2018).
44. Sirico, A. et al. Mechanical characterization of cement-based materials containing biochar from gasification. *Construct. Build. Mater.* **246**, 118490 (2020).
45. Patel, R., Stobbs, J. & Acharya, B. Study of biochar in cementitious materials for developing green concrete composites. *Sci. Rep.* **15**(1), 22192 (2025).
46. Cosentino, I., Restuccia, L., Ferro, G. A. & Tulliani, J. M. Type of materials, pyrolysis conditions, carbon content and size dimensions: the parameters that influence the mechanical properties of biochar cement-based composites. *Theor. Appl. Fract. Mech.* **103**, 102261 (2019).
47. Ahmad, W., Veeraghantla, V. S. S. C. S. & Byrne, A. Advancing sustainable concrete using biochar: experimental and modelling study for mechanical strength evaluation. *Sustainability* **17**(6), 2516 (2025).
48. Gupta, S., Kua, H. W. & Dai Pang, S. Effect of biochar on mechanical and permeability properties of concrete exposed to elevated temperature. *Constr. Build. Mater.* **234**, 117338 (2020).
49. Ahmad, S., Khushnood, R. A., Jagdale, P., Tulliani, J. M. & Ferro, G. A. High performance self-consolidating cementitious composites by using micro carbonized bamboo particles. *Mater. Des.* **76**, 223–229 (2015).

50. Galano, S. et al. Innovative approaches to enhancing concrete compressive strength: an extensive investigation of biochar-embedded and self-repairing techniques. *J. Mater. Civil Eng.* **37**(5), 04025112 (2025).
51. Samal, K. et al. Design of faecal sludge treatment plant (FSTP) and availability of its treatment technologies. *Energy Nexus* **7**, 100091 (2022).
52. Standard, I. Methods of physical tests for hydraulic cement. *Bureau of Indian Standards (BIS), New Delhi, India, IS*, 4031-1988. (1988).
53. Debieb, F. & Kenai, S. The use of coarse and fine crushed bricks as aggregate in concrete. *Constr. Build. Mater.* **22**(5), 886–893 (2008).
54. Standard, I. Methods of test for aggregates for concrete. *Part IV mechanical properties, IS*, *2386*. (1963).
55. Lehmann, J. & Joseph, S. Biochar for environmental management: An introduction. In *Biochar for Environmental Management* 1–13 (Routledge, 2015).
56. Abed Hussein, B. et al. Production, structural properties nano biochar and effects nano biochar in soil: a review. *Egypt. J. Chem.* **65**(12), 607–618 (2022).
57. American Society for Testing and Materials. *Standard Specification for Coal Fly Ash and Raw or Calcined Natural Pozzolan for Use in Concrete* (ASTM international, 2008).
58. Yasir, M., Di Summa, D., Ruscica, G., Natali Sora, I. & Savi, P. Shielding properties of cement composites filled with commercial biochar. *Electronics* **9**(5), 819 (2020).
59. Standard, I. *Is 10262: Guidelines for Concrete Mix Design Proportioning* (Indian Standard, 2009).
60. Berodier, E. S. K. S. G. & Scrivener, K. Understanding the filler effect on the nucleation and growth of C-S-H. *J. Am. Ceram. Soc.* **97**(12), 3764–3773 (2014).
61. Feng, X., & Clark, B. Evaluation of the physical and chemical properties of fly ash products for use in Portland cement concrete. (2011).
62. Concrete, C., Cabinets, M., & Rooms, M. Standard test method for length change of hardened hydraulic-cement mortar and. *Current 4* 1-7 (2010).
63. Nandana, P. S., Riyana, M. S., Parvathy, V., Abhijith, K. S., & Muhammad Ameen, K. Property enhancement of two-stage concrete incorporating agricultural wastes. In *International Conference on Advances in Materials, Modeling, and Analysis for Sustainable and Resilient Infrastructure* (pp. 547-558). Singapore: Springer Nature Singapore (2025).
64. American society for testing and materials. Standard test method for density, absorption, and voids in hardened concrete. West Conshohocken, PA, USA: ASTM (2006).
65. Mohanraj, R. & Sharma, G. Analysis of fly ash-based PPC concrete with nano-SiO_2 particles by rebound hammer and UPVT methods. *Procedia Struct. Integr.* **70**, 82–88 (2025).
66. Mensah, R. A. et al. Biochar-added cementitious materials—A review on mechanical, thermal, and environmental properties. *Sustainability* **13**(16), 9336 (2021).
67. Tiwari, R., Anand, S. & Mehra, P. Experimental assessment for compressive strength of sludge biochar added mortar. *Environ. Conserv. J.* https://doi.org/10.36953/ecj.34493162 (2025).
68. Famili, H., Saryazdi, M. K. & Parhizkar, T. Internal curing of high strength self consolidating concrete by saturated lightweight aggregate-effects on material properties. *Int. J. Civ. Eng.* **10**(3), 210–221 (2012).
69. Olaiya, B. C., Lawan, M. M., Olonade, K. A. & Segun, O. O. An overview of the use and process for enhancing the pozzolanic performance of industrial and agricultural wastes in concrete. *Discov. Appl. Sci.* **7**(3), 164 (2025).
70. Justs, J., Wyrzykowski, M., Winnefeld, F., Bajare, D. & Lura, P. Influence of superabsorbent polymers on hydration of cement pastes with low water-to-binder ratio: A calorimetry study. *J. Therm. Anal. Calorim.* **115**(1), 425–432 (2014).
71. Li, S. et al. Effect and mechanisms of biochar particle size and dosage on the hydration process and mechanical properties of cementitious materials. *Construct. Building Mater.* **472**, 140931 (2025).
72. Gupta, S., Krishnan, P., Kashani, A. & Kua, H. W. Application of biochar from coconut and wood waste to reduce shrinkage and improve physical properties of silica fume-cement mortar. *Constr. Build. Mater.* **262**, 120688 (2020).
73. Odimegwu, T. C., Zakaria, I., Abood, M. M., Nketsiah, C. B. K. & Ahmad, M. Review on different beneficial ways of applying alum sludge in a sustainable disposal manner. *Civ. Eng. J.* **4**(9), 2230–2241 (2018).
74. Sirico, A. et al. Biochar from wood waste as additive for structural concrete. *Constr. Build. Mater.* **303**, 124500 (2021).
75. Lorenzoni, R. et al. Microstructure analysis of cement-biochar composites. *Mater. Struct.* **57**(8), 175 (2024).
76. Paula, R. et al. Analysis of biochar-cement composites by SEM/EDS: interfacial interactions and effects on mechanical strength. *C* **11**(3), 45 (2025).
77. Muthu, M., Kumar, S. & Sadowski, Ł. Performance of pozzolan-based reactive magnesia cement mixes against sulphate attack. *Appl. Sci.* **13**(19), 11012 (2023).
78. Kunther, W., Ferreiro, S. & Skibsted, J. Influence of the Ca/Si ratio on the compressive strength of cementitious calcium–silicate–hydrate binders. *J. Mater. Chem. A* **5**(33), 17401–17412 (2017).
79. Sathawane, S. H., Vairagade, V. S. & Kene, K. S. Combine effect of rice husk ash and fly ash on concrete by 30% cement replacement. *Procedia Eng.* **51**, 35–44 (2013).
80. Joel, S. Compressive strength of concrete using fly ash and rice husk ash: A review. *Civ. Eng. J.* **6**(7), 1400–1410 (2020).

81. Siddique, R. & Klaus, J. Influence of metakaolin on the properties of mortar and concrete: A review. *Appl. Clay Sci.* **43**(3–4), 392–400 (2009).
82. Yang, X., Lin, R. S., Han, Y. & Wang, X. Y. Behavior of biochar-modified cementitious composites exposed to high temperatures. *Materials* **14**(18), 5414 (2021).
83. Gomes, S. D. C., Zhou, J. L., Zeng, X. & Long, G. Water treatment sludge conversion to biochar as cementitious material in cement composite. *J. Environ. Manage.* **306**, 114463 (2022).
84. Shi, G. et al. A new perspective toward sludge biochar with adsorbed heavy metals for cement mortar production. *Environ. Technol. Innov.* **37**, 104013 (2025).
85. Wijeyawardana, P. et al. Performance of biochar mixed cement paste for removal of Cu, Pb and Zn from stormwater. *Environ. Res.* **232**, 116331 (2023).
86. Chen, X. et al. Sludge biochar as a green additive in cement-based composites: Mechanical properties and hydration kinetics. *Constr. Build. Mater.* **262**, 120723 (2020).
87. Li, G. et al. Stabilization/solidification of heavy metals and PHe contaminated soil with β-cyclodextrin modified biochar (β-CD-BC) and Portland cement. *Int. J. Environ. Res. Public Health* **19**(3), 1060 (2022).

Authors and Affiliations

Raghuvesh Tiwari[1] · Priyansha Mehra[1] · Shaik Hussain[2] · Sanchit Anand[1]

✉ Raghuvesh Tiwari
Raghuvesh.tiwary@jaipur.manipal.edu

✉ Priyansha Mehra
priyansha.mehra@jaipur.manipal.edu

1 Department of Civil Engineering, Manipal University Jaipur, Jaipur, Rajasthan 303007, India

2 Trenchless Technology Center, Louisiana Tech University, Ruston, L.A 71272, USA